Supplementary Information (SI) for Catalysis Science & Technology.
This journal is © The Royal Society of Chemistry 2024

An Exploration of the Electrocatalytic Activity of Nickel Boride Nanocrystals in the Oxidation of 5-HMF

Jennifer Hong[a,b], Matteo Miola[a], Dominic Gerlach[b], Marc C. A. Stuart[c], Petra Rudolf[b], Dulce M. Morales[a], Loredana Protesescu[b], Paolo P. Pescarmona[a,*]

[a] Engineering and Technology Institute Groningen (ENTEG), University of Groningen, 9747AG Groningen, Netherlands

[b] Zernike Institute for Advanced Materials, University of Groningen, 9747AG Groningen, Netherlands

[c]Groningen Biomolecular Sciences and Biotechnology Institute, University of Groningen, 9747AG Groningen, Netherlands

Supporting Information

Table of Contents

Table S1. Reported Ni_xB-based electrocatalyst studied for the electrooxidation of 5-HMF.

Material	Catalyst loading (mg/cm^2)	HMF concentration (mM)	pH	Potential (V vs RHE)	Reaction time (h)	HMF conversion (%)	Yield (%)	$n_{product}$ (mmol)	FE (%)	TOF [a]	Ref.
Ni_3B-NCs@CP	0.05	100	13.9	1.8	3	70	FDCA ~33 HMFCA~5 FFCA~7	n_{FDCA} ~ 0.33 n_{HMFCA} ~0.05 n_{FFCA} ~0.07	94-100	16	This work
	0.05	100	13.9	1.5	3	60	FDCA ~32 HMFCA~8 FFCA~8	n_{FDCA} ~ 0.32 n_{HMFCA} ~0.08 n_{FFCA} ~0.08	100	16	
	0.05	100	13.9	1.8	8	97	FDCA ~54 HMFCA~4 FFCA~8	n_{FDCA} ~ 0.54 n_{HMFCA} ~0.04 n_{FFCA} ~0.08	47	9.1	
	0.05	100	12.9	1.8	3	37	FDCA ~3 DFF~4.5 FFCA~18.8	n_{FDCA} ~ 0.03 n_{DFF} ~0.045 n_{FFCA} ~0.188	100	6.8	
	0.15	100	12.9	1.8	3	37	FDCA ~2.9 DFF~3.9 FFCA~18.5	n_{FDCA} ~ 0.029 n_{DFF} ~0.039 n_{FFCA} ~0.185	100	2.2	
	0.75	100	12.9	1.8	3	39.3	FDCA ~4.8 DFF~4.1 FFCA~16.9	n_{FDCA} ~ 0.048 n_{DFF} ~0.041 n_{FFCA} ~0.169	100	0.5	
Ni_xB/NF	1	10	13.9	1.45	50 min	99	98.5	0.0985	~100	0.709	1
NiB_x/NF	2.47	10	13.9	0.6 vs SHE	1h 40 min	99	99	0.396	99.5	0.57 [b]	2
NiB_x-P_y/CP (amorphous)	4	10	12.9	1.46	Charge passed: 35 C	97 - 99	FDCA ~60-80 FFCA ~9.8-35		80-92	0.128 [c]	3

[a] $$Turnover\ frequency\ (TOF) = \frac{n_{e(FDCA)} \cdot n_{FDCA} + n_{e(FFCA)} \cdot n_{FFCA} + n_{e(HMFCA)} \cdot n_{HMFCA} + n_{e(DFF)} \cdot n_{DFF}}{m_{Ni_xB} \cdot t}$$

where $n_{e(P)}$ (P = FDCA, FFCA, HMFCA or DFF) is the number of electrons required to oxidize 5-HMF to product P ($n_{e(FDCA)}$ = 6, $n_{e(FFCA)}$ = 4, $n_{e(HMFCA)}$ = $n_{e(DFF)}$ = 2) and n_P is the mol of compound P (mmol). m_{Ni_xB} is the mass of the Ni_xB on the electrode (mg) and t is the reaction time (h).

[b] Assuming an electrode area of 1 cm^2 (the electrode area was not provided) and electrolyte volume of 40 mL (based on data on the caption in the supporting information).

[c] Assuming reaction time of 1 h and electrolyte volume of 10 mL (any information regarding reaction/measurement time and electrolyte volume were not provided).

Table S2. Reported Ni_xB-based electrocatalyst studied for the electrooxidation of 5-HMF.

Material	Catalyst loading (mg mg/cm^2)	HMF concentration (mM)	pH	Potential (V vs RHE)	Reaction time (h)	HMF conversion (%)	Yield (%)	FE (%)	Reference
NiFe@NF	N/A	50-100	13.9	1.478	0.2	99	FDCA ~92%	92	[4]
NiO/Ni(OH)$_2$	N/A	5	13.9	Chronopotentiometry 16 mA/cm^2	4	N/A	FDCA 71%	84	[5]
Ni_3S_2/NF	N/A	10	13.9	1.423	Charge passed 58 C	100	FDCA ~98	98	[6]
Ni_2P NPA/NF	N/A	10	13.9	1.423	2.5	100	FDCA selecttivity ~100	98	[7]
Hp-Ni	75	10	13.9	1.423	Charge passed 58 C	100	FDCA ~95	98	[8]
NiP-Al_2O_3/NF	1.2	10	13.9	1.45	3.5	98.2	FDCA selectivity ~99.6	N/A	[9]
Branched Ni NPs	0.35	N/A	12.9	1.43	N/A	N/A	N/A	N/A	[10]
Ni_3N@C	N/A	10	13.9	1.45	Charge passed 174	100	98	99	[11]
NiO-Co_3O_4	N/A	10	13.9	1.45	0.5	100	98.5	100	[12]
h-Ni(OH)$_2$	0.625	10	13.9	Chronopotentiometry 20 mA/cm^2	3.3	98.8	FDCA selectivity ~98.5	94.9	[13]
t-NiCo-MOF	1.05-1.55	10	13.9	N/A	Charge passed 58	100	FDCA ~100	98	[14]
NiSe@NiO$_x$/NF	2.1	10	13.9	1.423	2	100	FDCA ~99	99	[15]
NiO NPs	N/A	10	7.23	1.5-1.7	Charge passed 29	90	FDCA ~30	70	[16]
Au-NiO	N/A	10	13.9	0.4 V vs Ag/AgCl	5	N/A	N/A	99	[17]
NiOOH	N/A	10	12.9	1.47	4.7	99.8	FDCA ~96	96	[18]
NiCoBDC-NF	N/A	10	12.9	1.55	4	N/A	FDCA selectivity ~99	78	[19]
β-$Co_{0.1}Ni_{0.9}$(OH)$_2$	N/A	10	13.9	N/A	N/A	100	FDCA ~96	~93	[20]
NiO/carbon felt	0.375	0.2 mM	11	1.44	12	100	FDCA 98	N/A	[21]
NiFe LDH	N/A	10 - 100	13.9	1.23 – 1.43	0.5 - 10	91 - 99	FDCA 90 - 98	77 - 99	[22]
Ni MOF	0.5	50	13.9	1.5	Charge passed ~58 C	100	FDCA ~70	98	[23]
Ni(NS)/CP	N/A	5	13.9	1.33	1	99.7	FDCA~99.4	N/A	[24]
NiCoFe LDHs	0.532	10	13.9	1.54	1	95.5	FDCA ~84.9	90	[25]
$NiCo_2O_4$	N/A	5	13.9	1.5	~0.9	99.6	FDCA ~90.4	87.5	[26]
Ni_xSe_y/NiFeLDH@NF	7.2	10	13.9	1.423	> 1	99.6	FDCA ~99.3	98.9	[27]
NiCoS	N/A	10	13.9	1.45	0.67	99.1	FDCA	96.4	[28]

							~97.1		
d-NiFe LDH	N/A	10	13.9	1.48	5	95.5	FDCA ~96.8	84.5	[29]
CoFe LDH@NiFe LDH	N/A	10	13.9	1.4	> 3	100	FDCA ~100	99.8	[30]
NiVCo-LDH	N/A	10	13.9	1.376	Charge passed ~58 C	100	FDCA ~99.7	97	[31]
NiCu NTs	16.67	20	13.9	1.42	2	100	FDCA ~99	96.4	[32]
RuNiO	3.2 wt%	50	7	1.3-1.8	Charge passed ~90 C	72.4	DFF ~42.5	43.3	[33]
Mo-$Ni_{0.85}Se$	N/A	10	13.9	1.4	2	100	FDCA ~99	99	[34]
Pt-$Ni(OH)_2$	0.2	50	13.9	N/A	N/A	100	FDCA ~96	98.7	[35]
Co-Ni_3S_2	N/A	50	13.9	1.45	0.3	100	FDCA ~100	99.1	[36]
$Ni(OH)_2$-NiFeP	N/A	10	13.9	1.55	Charge passed ~85 C	100	FDCA ~99	94	[37]
Ni_2P-NiCoP	1.8	5	12.9	1.45	Charge passed ~60 C	100	FDCA ~98.1	97.6	[38]
NiS_x-Ni_2P	N/A	10	13.9	1.46	Charge passed ~90 C	100	98.5	95.1	[39]
FeP-$NiMoP_2$	N/A	10	13.9	1.40	1.8	100	FDCA ~99.2	99	[40]
MoS_2-Ni_3S_2	N/A	50	13.9	1.35-1.7	2.6-8	N/A	FDCA ~95	95	[41]

Table S3. Carbon balance of 5-HMF oxidation in 0.1 M KOH (pH 12.9) after 3 h of chronoamperometry at 1.8 V vs RHE

Electrode	Carbon balance (%)
Ni-NCs@CP	91
Ni_3B-NCs@CP	95
Ni_2B-NCs@CP	95

Table S4. Carbon balance of 5-HMF oxidation in 1.0 M KOH (pH 13.9) after 3 h of chronoamperometry at 1.8 V vs RHE

Electrode	Carbon balance (%)
Ni-NCs@CP	66
Ni_3B-NCs@CP	73
	58[a]
Ni_2B-NCs@CP	75

[a] Carbon balance of electrochemical oxidation of 5-HMF with Ni_3B-NCs@CP at 1.8 V vs RHE for 8 h.

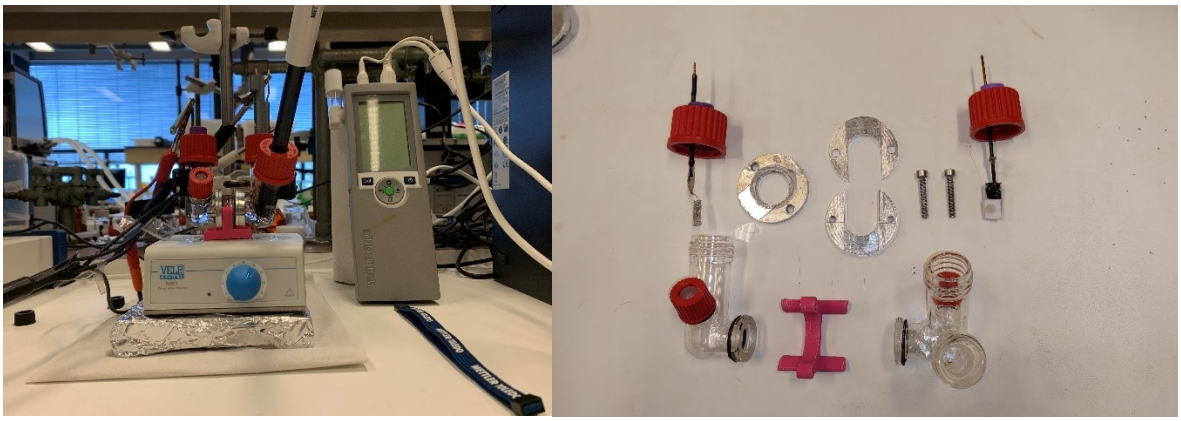

Figure S1. Images of two compartment H-type cell with a three-electrode configuration equipped with pH meter.

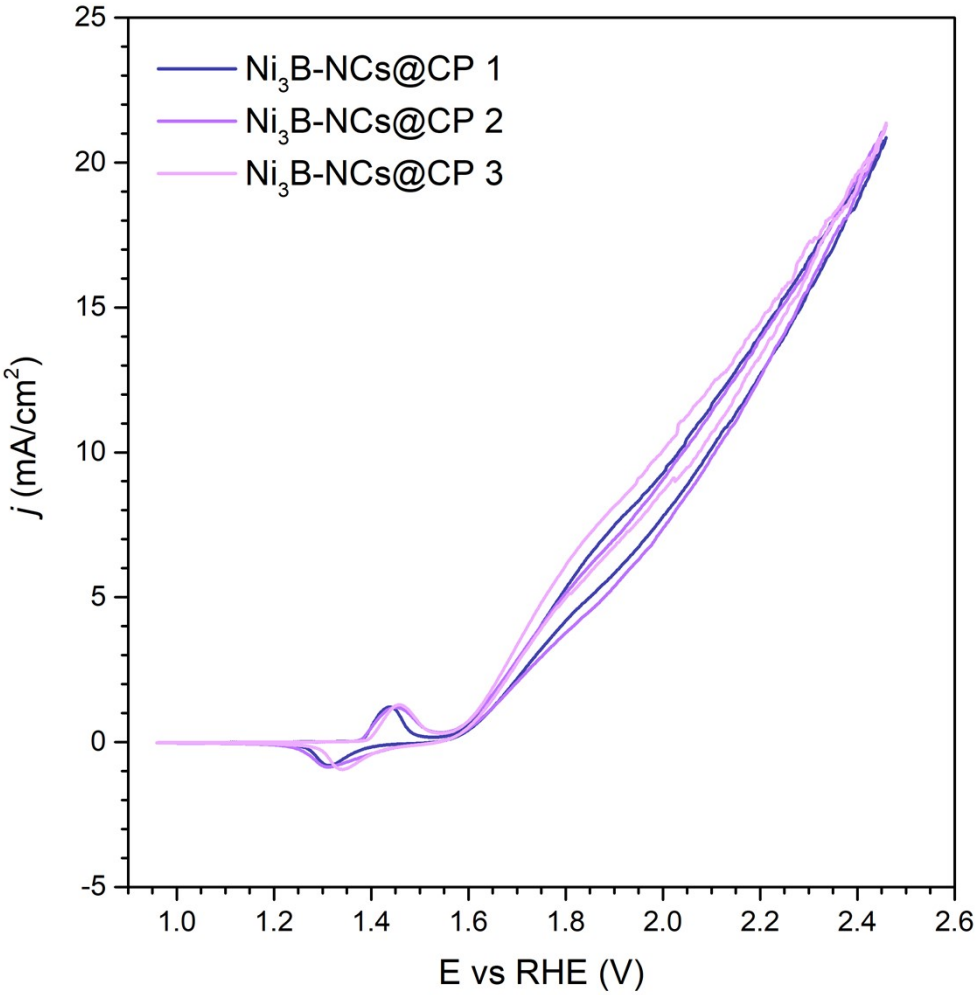

Figure S2. Reproducibility test of the Ni_3B-NCs@CP (Ni_3B NC loading 0.05 mg/cm^2) cyclic voltammetry at 10 mV/s in 0.1 M KOH (pH 12.9).

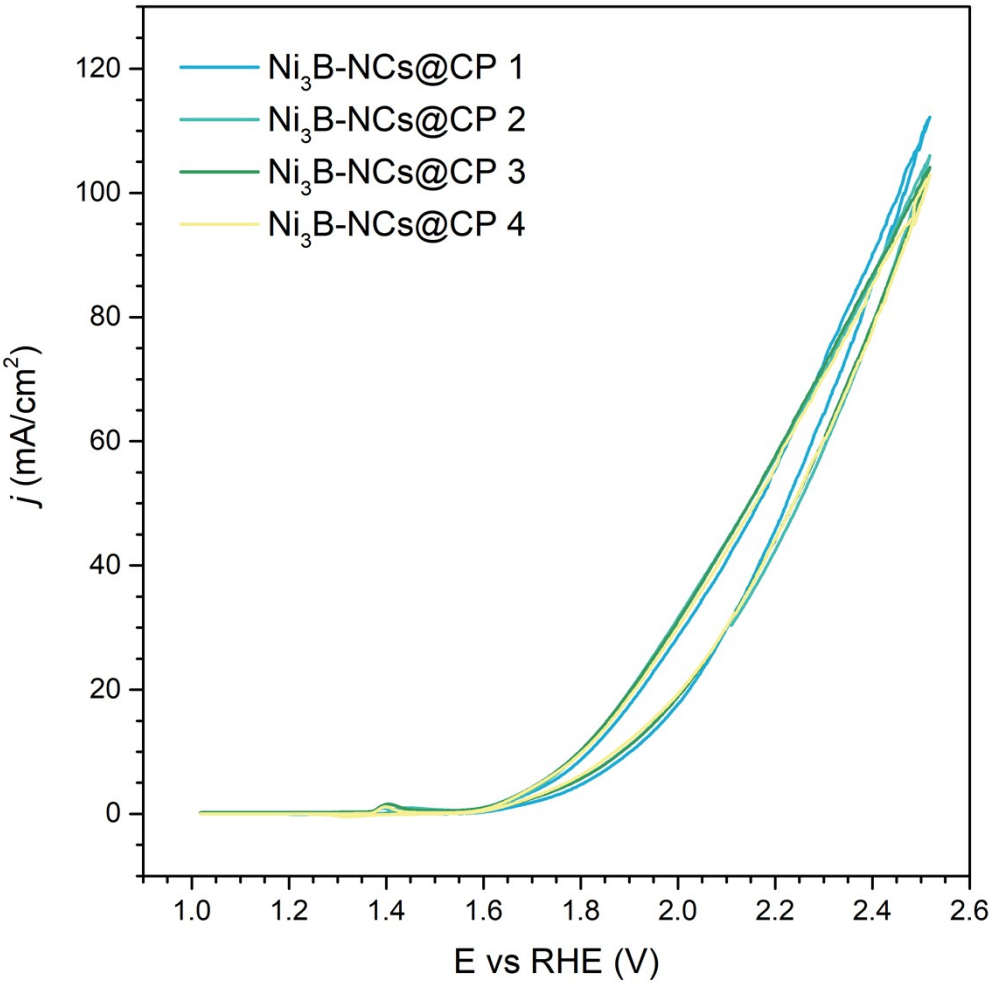

Figure S3. Reproducibility test of the Ni_3B-NCs@CP (Ni_3B NC loading 0.05 mg/cm^2) cyclic voltammetry at 10 mV/s in 1 M KOH (pH 13.9)

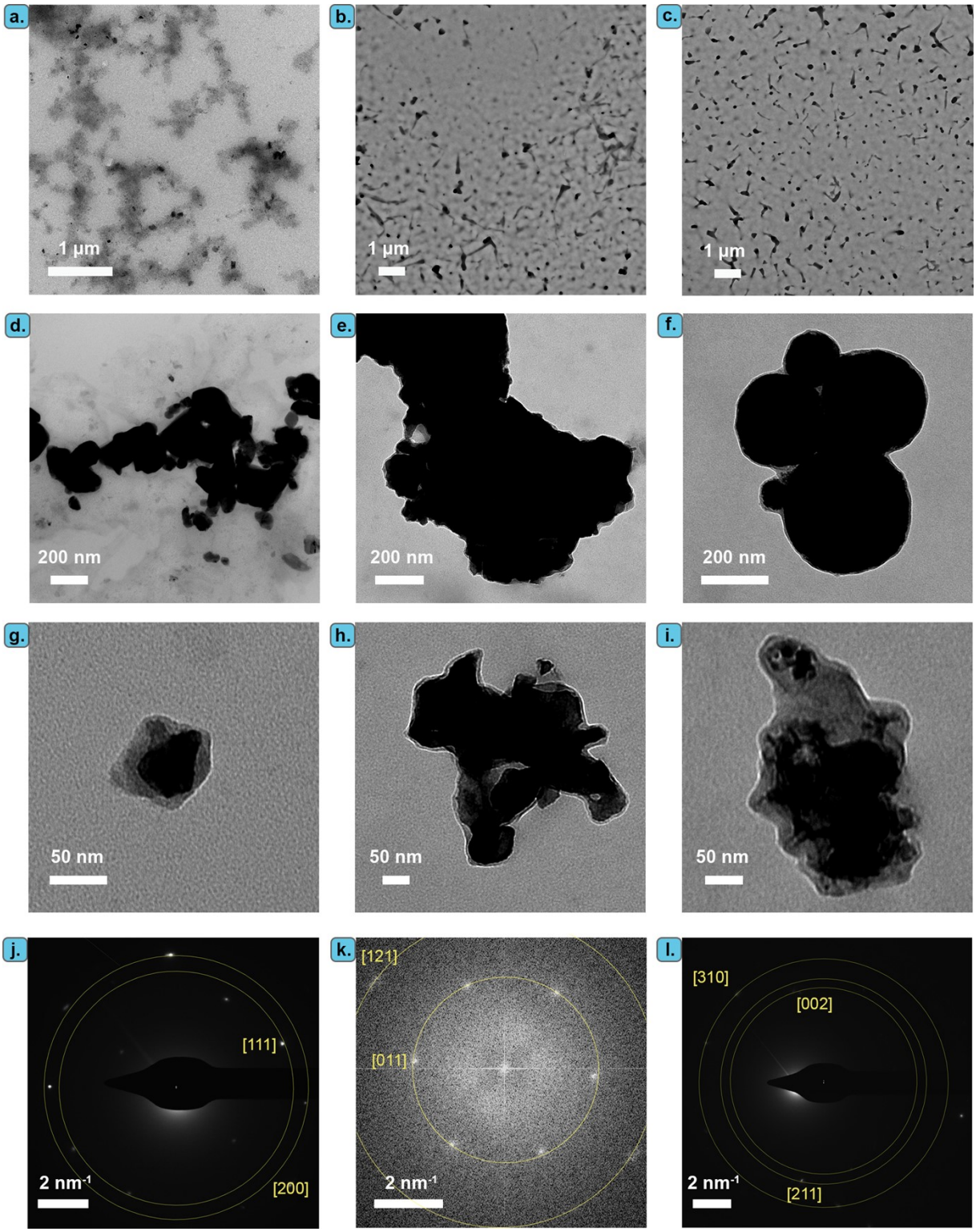

Figure S4. TEM images of (a, d, g) Ni NCs mixed with Nafion, (b, e, h) Ni_3B NCs mixed with Nafion, and (c, f, i) Ni_2B NCs mixed with Nafion. Selected area electron diffraction (SAED) of (j) Ni NCs mixed with Nafion, in which [111] corresponds to the peak at 2θ = 45 ° and [200] corresponds to the peak at 2θ = 52 ° in the XRD pattern in Fig. 2a; (k) Fast Fourier Transform (FFT) of Ni_3B NCs mixed with Nafion, in which [011] corresponds to the peak at 2θ = 24 ° and [121] corresponds to the peak at 2θ = 38 ° in the XRD pattern in Fig. 2b; (l) SAED of Ni_2B NCs mixed with Nafion, in which [002] corresponds to the peak at 2θ = 42 °, [211] corresponds to the

peak at 2θ = 46 ° and [310] corresponds to the peak at 2θ = 58 ° in the XRD pattern in Fig. 2c.

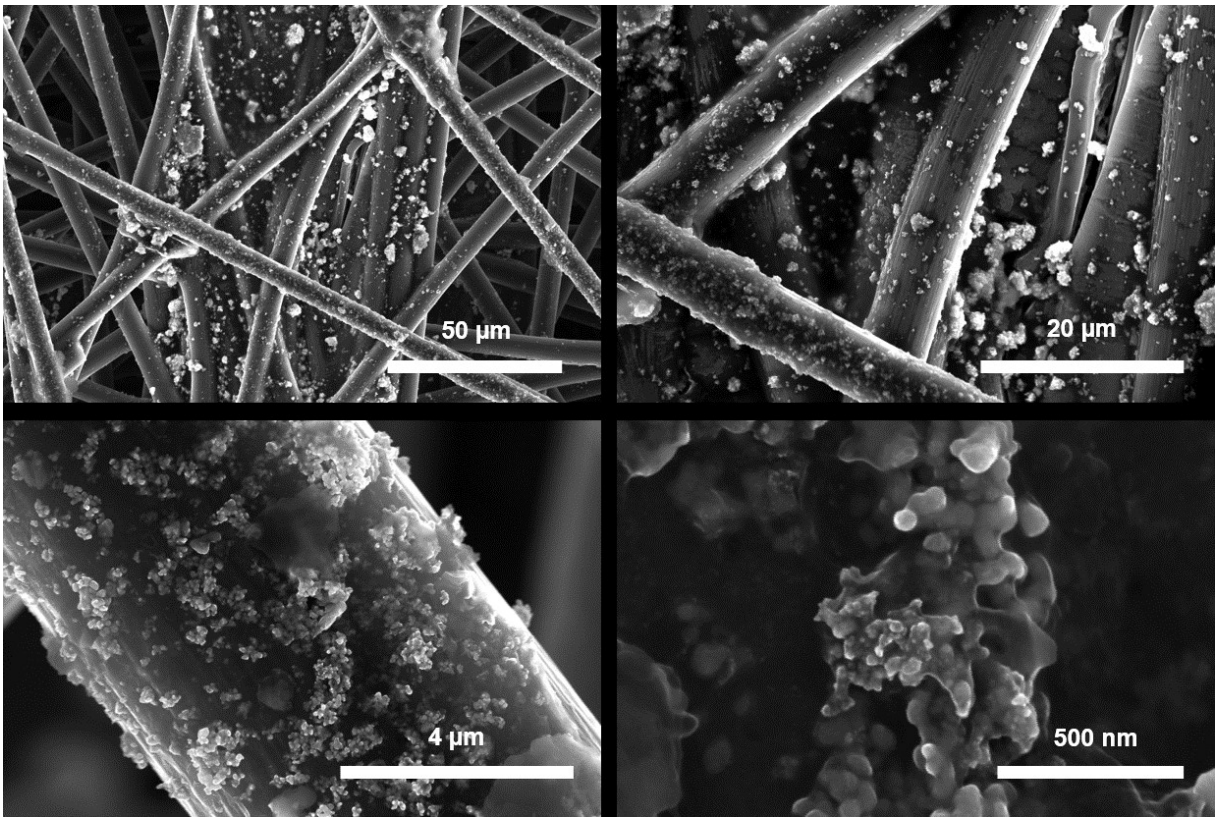

Figure S5. Scanning electron microscopy (SEM) images of Ni_3B-NCs@CP with catalyst loading of 0.15 mg/cm^2. Ni_3B NCs (3 mg) was dispersed in 1 mL of 0.1 M Nafion/DMSO solution. The mixture was stirred overnight at 90 C then sonicated for 45 minutes. 50 µL of the ink was dropcast onto 1x1 cm^2 carbon paper support and dried overnight at 70 C in vacuo.

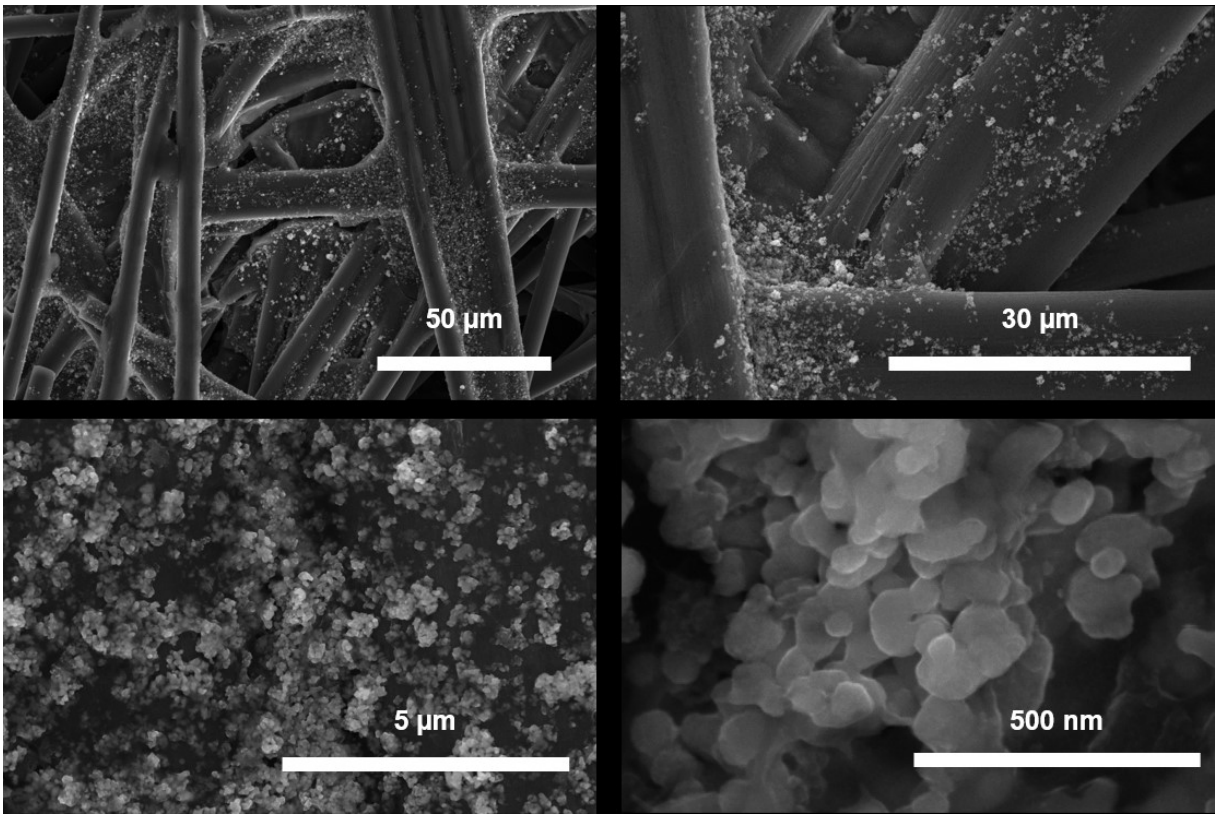

Figure S6. Scanning electron microscopy (SEM) images of Ni_3B-NCs@CP with catalyst loading of 0.75 mg/cm^2. Ni_3B NCs (15 mg) was dispersed in 1 mL of 0.1 M Nafion/DMSO solution. The mixture was stirred overnight at 90 C then sonicated for 45 minutes. 50 µL of the ink were then dropcast onto 1x1 cm^2 carbon paper support and dried overnight at 70 C in vacuo.

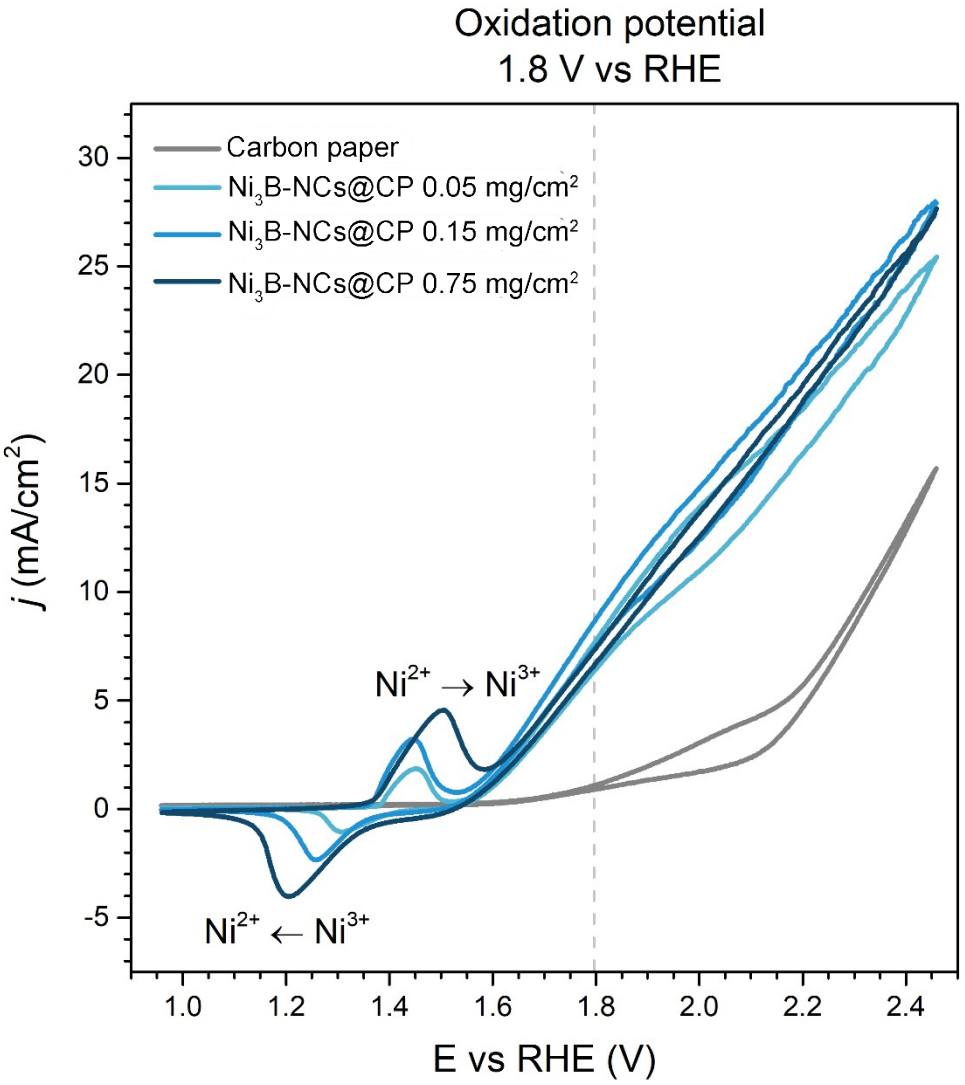

Figure S7. Cyclic voltammetry recorded at 10 mV/s of Ni_3B-NCs@CP with different catalyst loading in 0.1 M KOH (pH 12.9) in the absence 5-HMF.

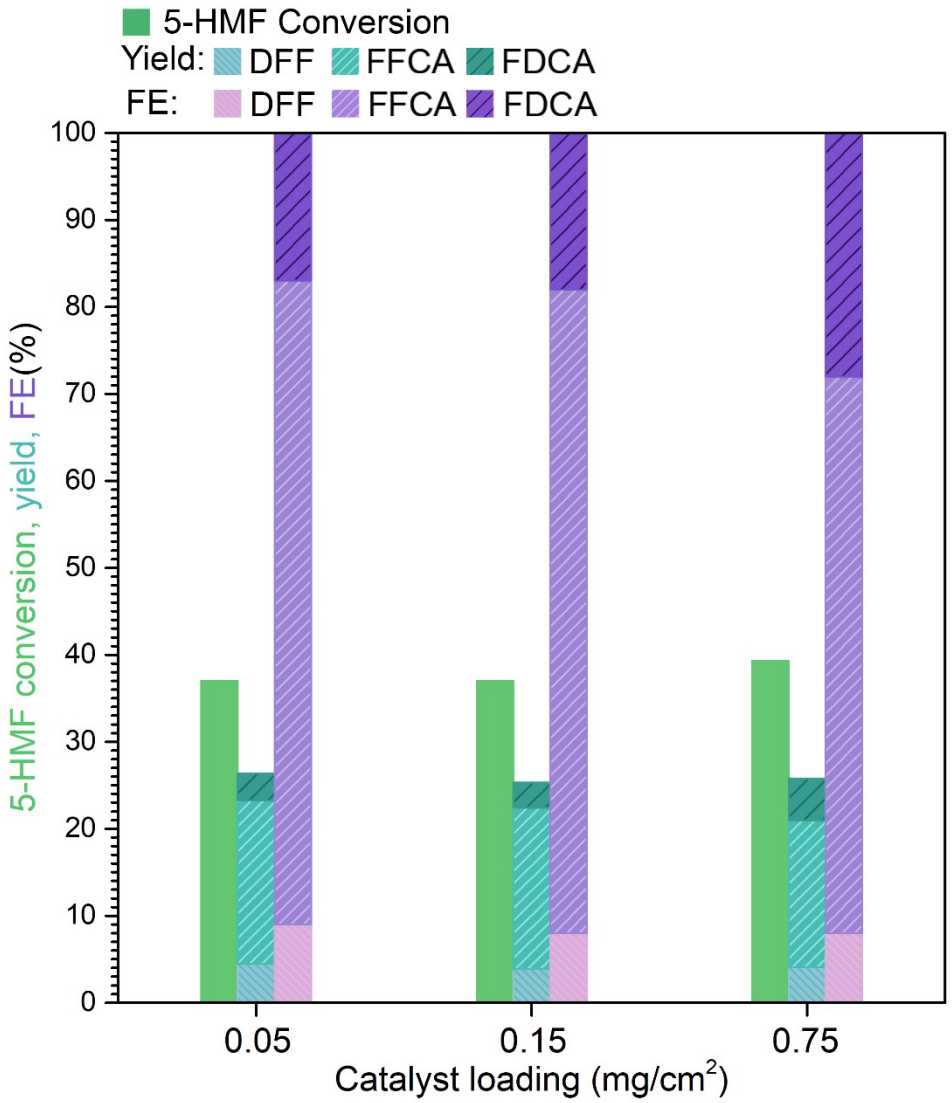

Figure S8. Conversion, yield, and Faradaic Efficiency (FE) of 5-HMF (100 mM) electrooxidation catalyzed by Ni_3B-NCs@CP with different catalyst loading at a constant potential 1.8 V vs RHE in 0.1 M KOH (pH 12.9).

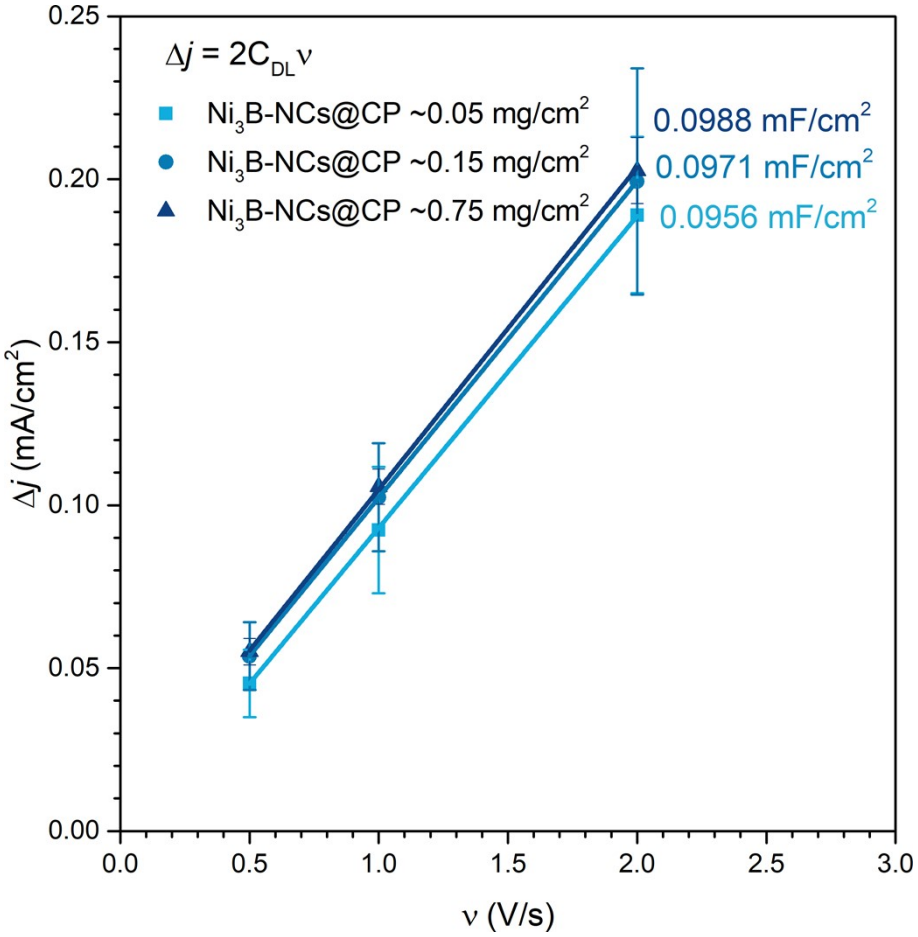

Figure S9. Difference between anodic to cathodic current density plotted against the scan rate. From the value of the slope of the plots ($2C_{DL}$), the double layer capacitance (C_{DL}) can be calculated.

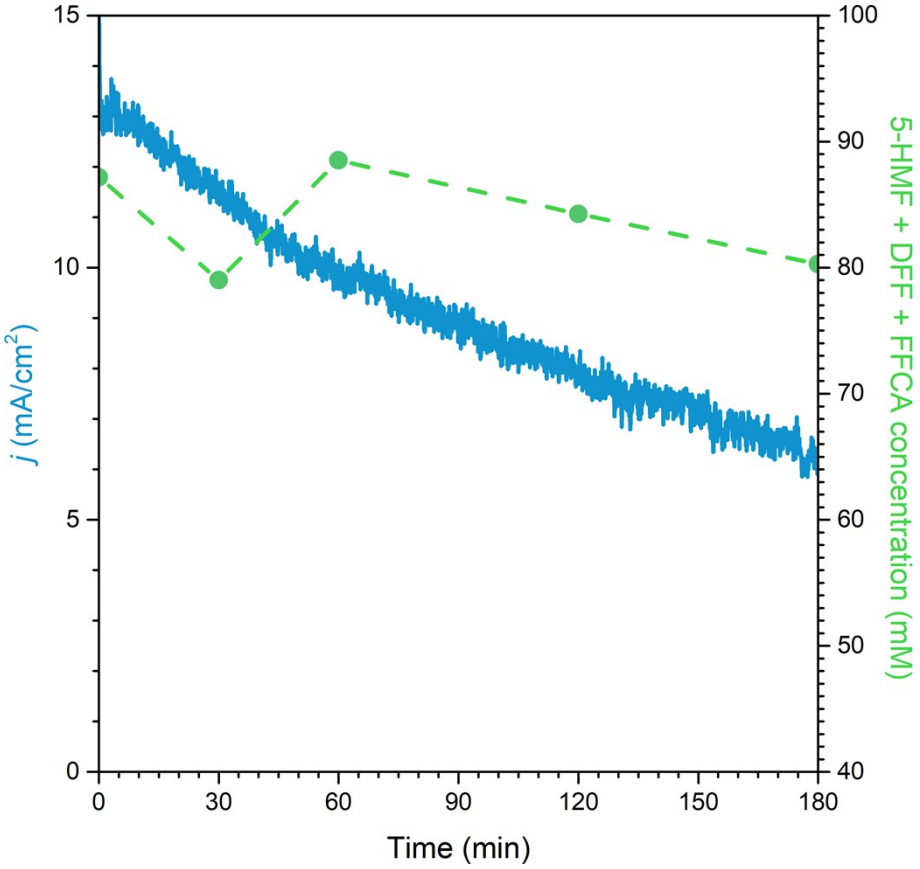

Figure S10. Current density and the sum of 5-HMF, DFF, and FFCA concentrations as function of electrolysis time obtained by chronoamperometry of Ni_3B-NCs@CP with catalyst loading 0.15 mg/cm^2 in 0.1 M KOH (pH 12.9).

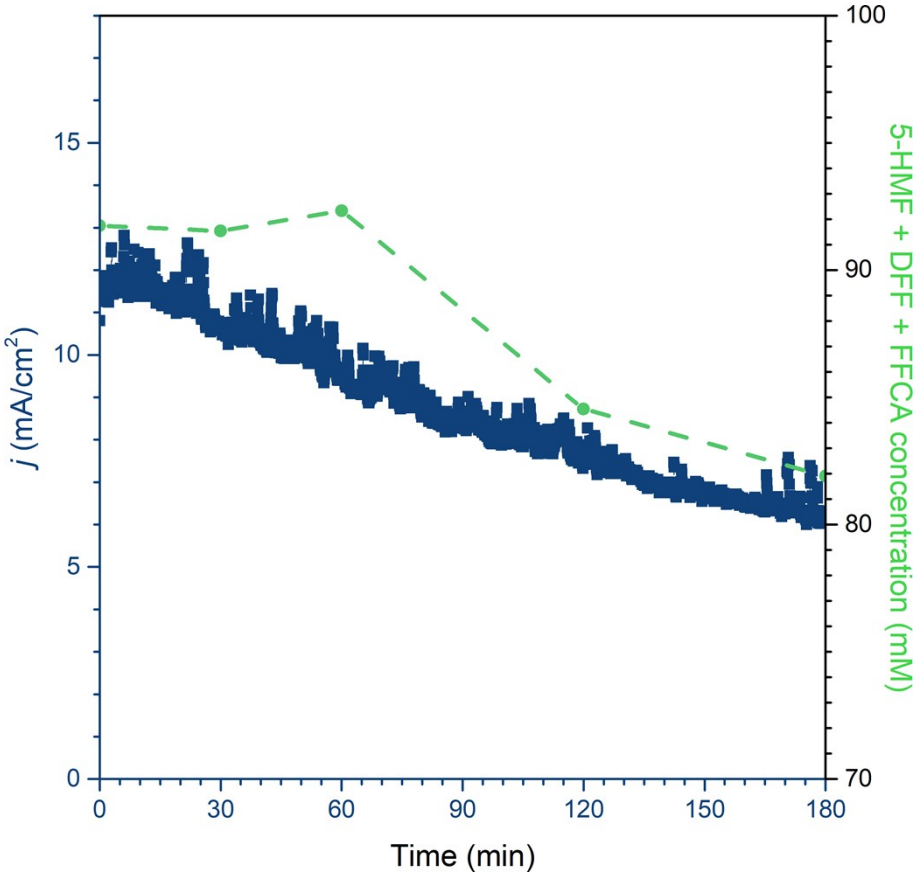

Figure S11. Current density and the sum of 5-HMF, DFF, and FFCA concentrations as function of electrolysis time obtained by chronoamperometry of Ni_3B-NCs@CP with catalyst loading 0.75 mg/cm^2 in 0.1 M KOH (pH 12.9).

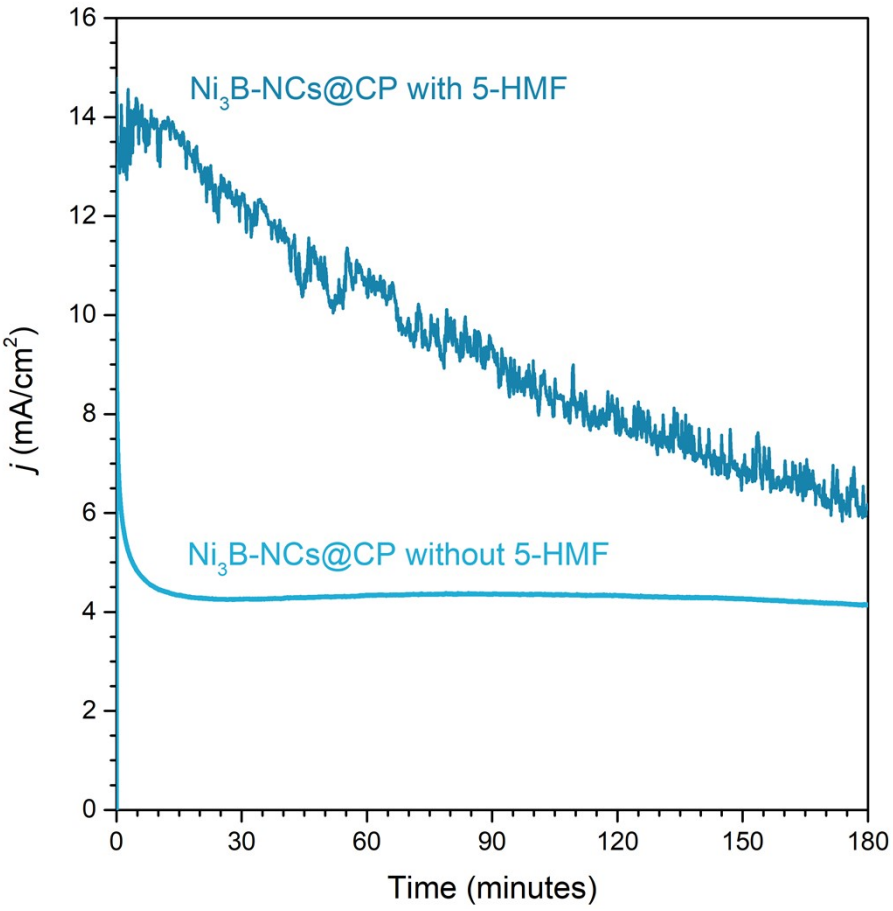

Figure S12. Chronoamperometry of Ni_3B-NCs@CP with catalyst loading 0.05 mg/cm^2 in 0.1 M KOH (pH 12.9) at 1.8 V vs RHE with 100 mM of 5-HMF and no 5-HMF.

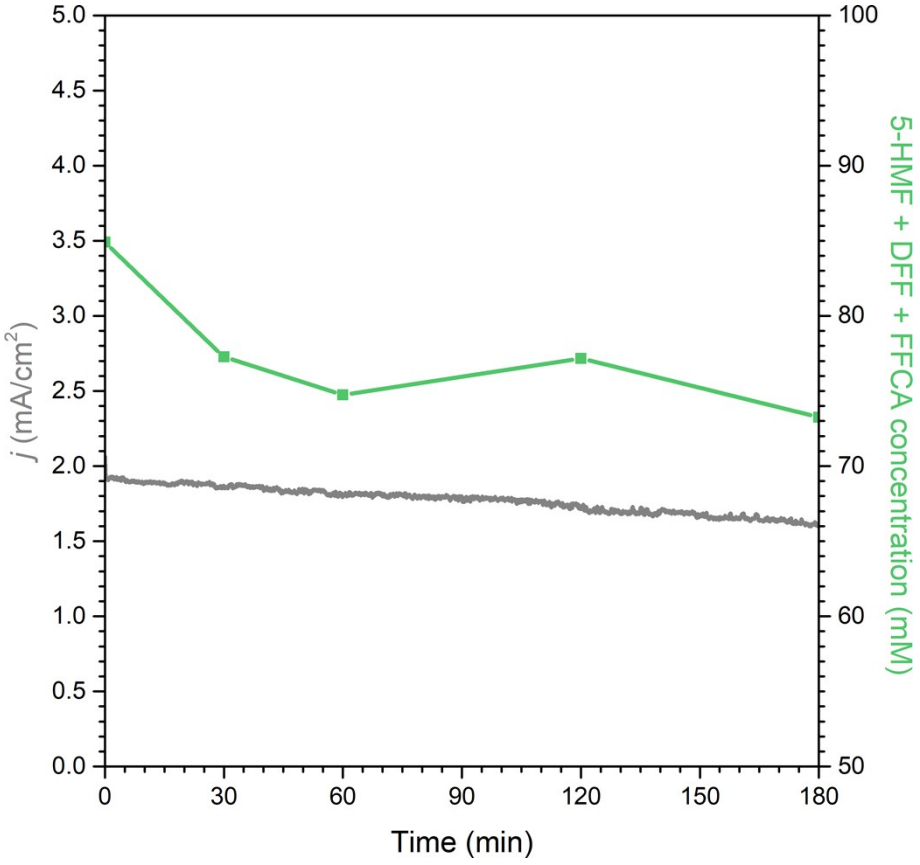

Figure S13. Current density and the sum of 5-HMF, DFF, and FFCA concentrations as function of electrolysis time obtained by chronoamperometry of carbon paper in 0.1 M KOH (pH 12.9).

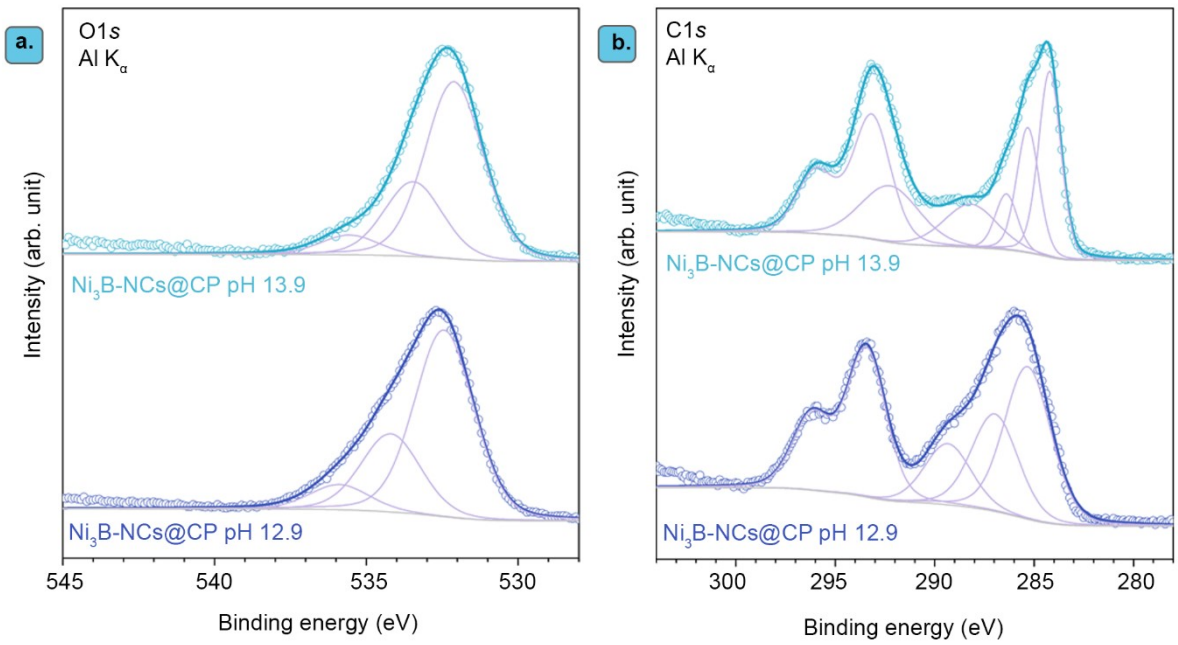

Figure S14. XPS spectra of the (a) O 1*s* and (b) C 1*s* core level regions of Ni_3B-NCs@CP post electrocatalytic test at pH 12.9 (purple), and at pH 13.9 (blue).

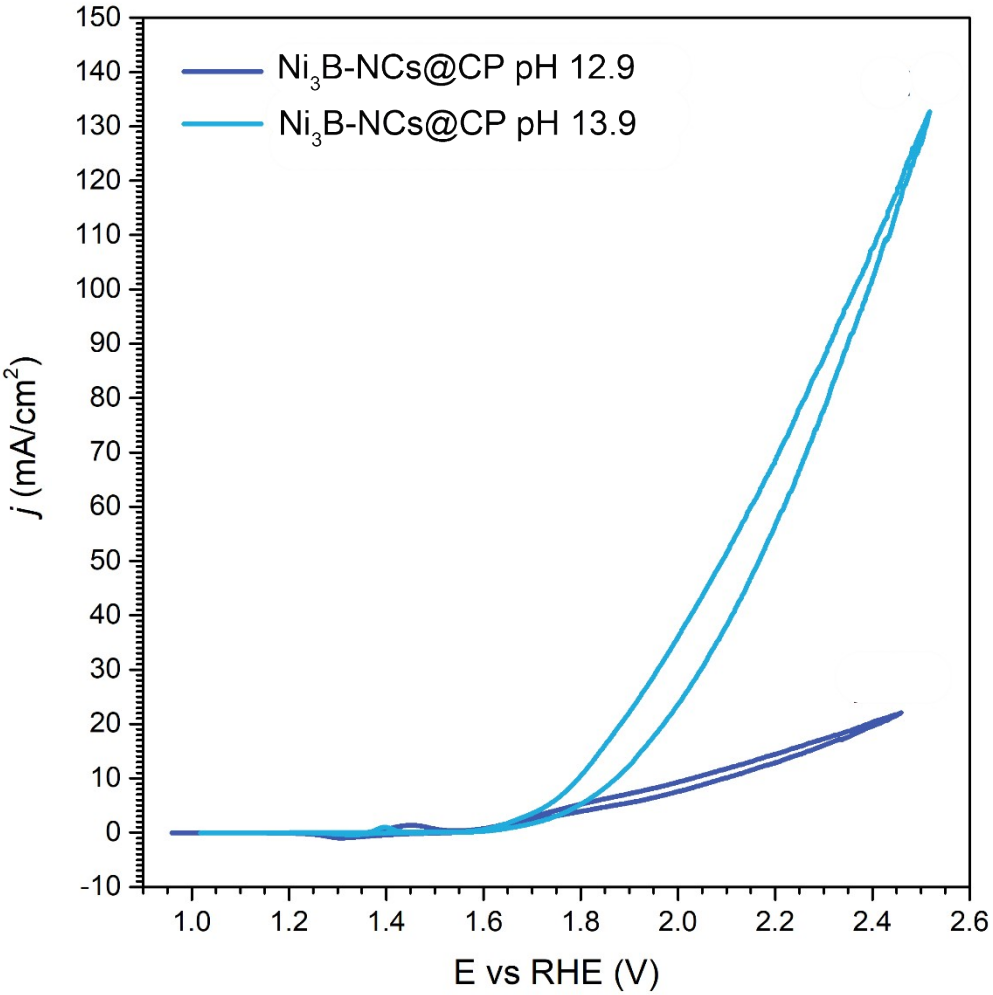

Figure S15. Cyclic voltammetry recorded with scan rate of 10 mV/S for Ni_3B-NCs@CP (0.05 mg/cm^2) measured at pH 12.9 (0.1 M KOH) and pH 13.9 (1.0 M KOH). These measurements were carried out in the absence of 5-HMF.

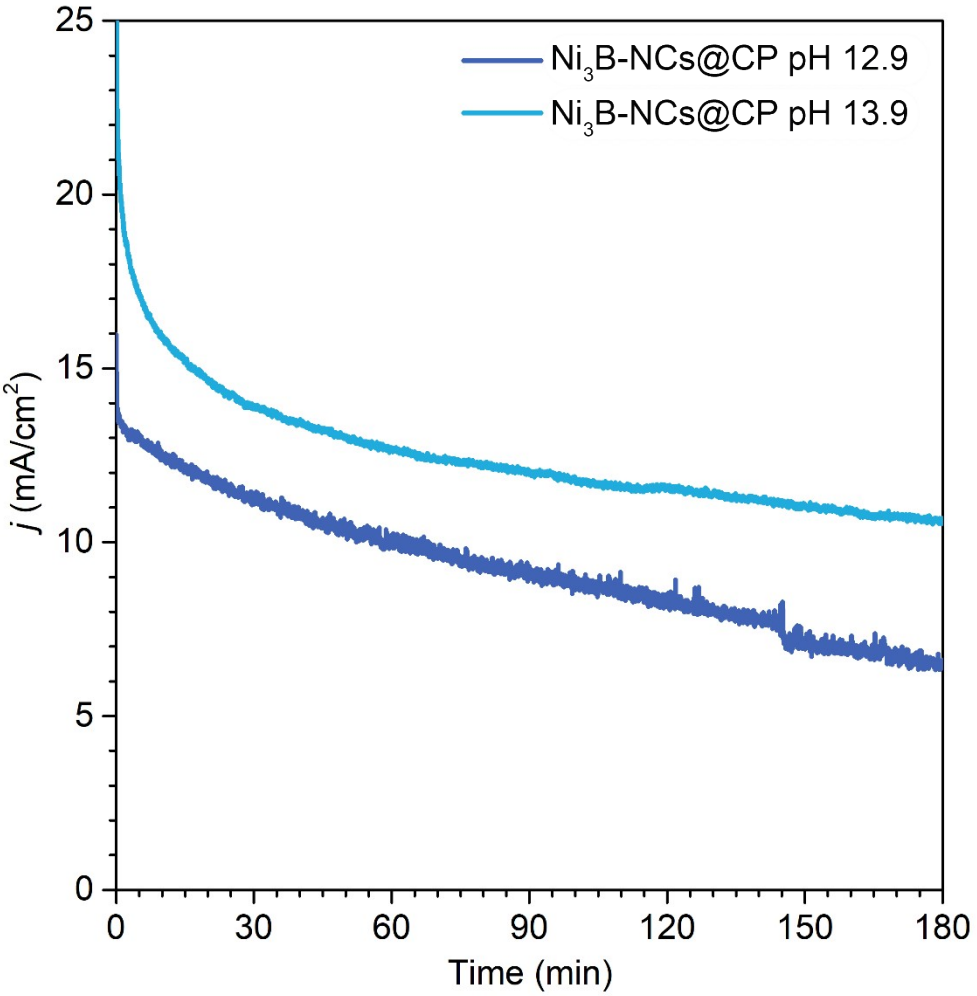

Figure S16. Chronoamperometry of Ni_3B-NCs@CP (0.05 mg/cm^2) conducted at constant potential 1.8 V vs RHE for 3 hours in the presence of 5-HMF (100 mM) at pH 12.9 (0.1 M KOH, dark blue line) and pH 13.9 (1.0 M KOH, light blue line).

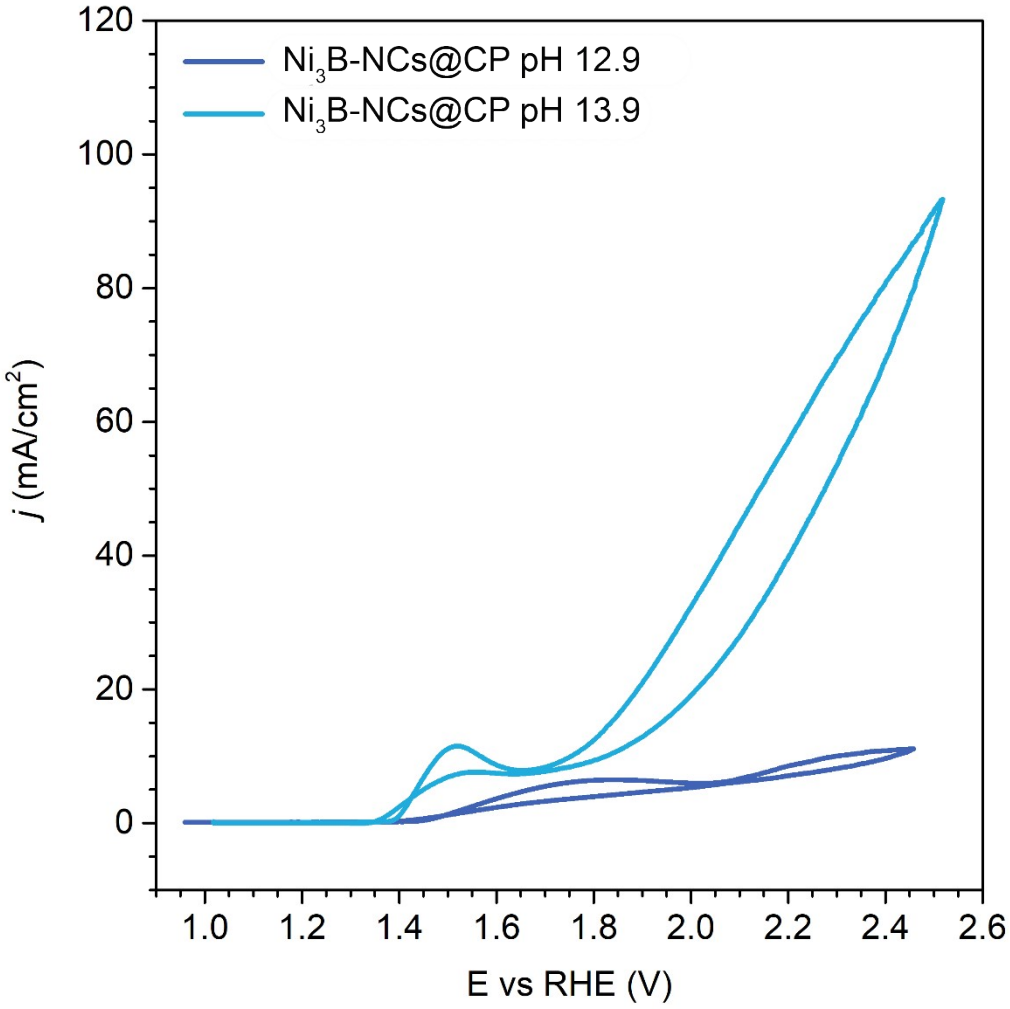

Figure S17. Cyclic voltammetry recorded with scan rate of 10 mV/S for Ni_3B-NCs@CP (0.05 mg/cm^2) measured at pH 12.9 (0.1 M KOH) and pH 13.9 (1.0 M KOH) after 3 hours of 5-HMF electrooxidation (chronoamperometry at 1.8 V vs RHE).

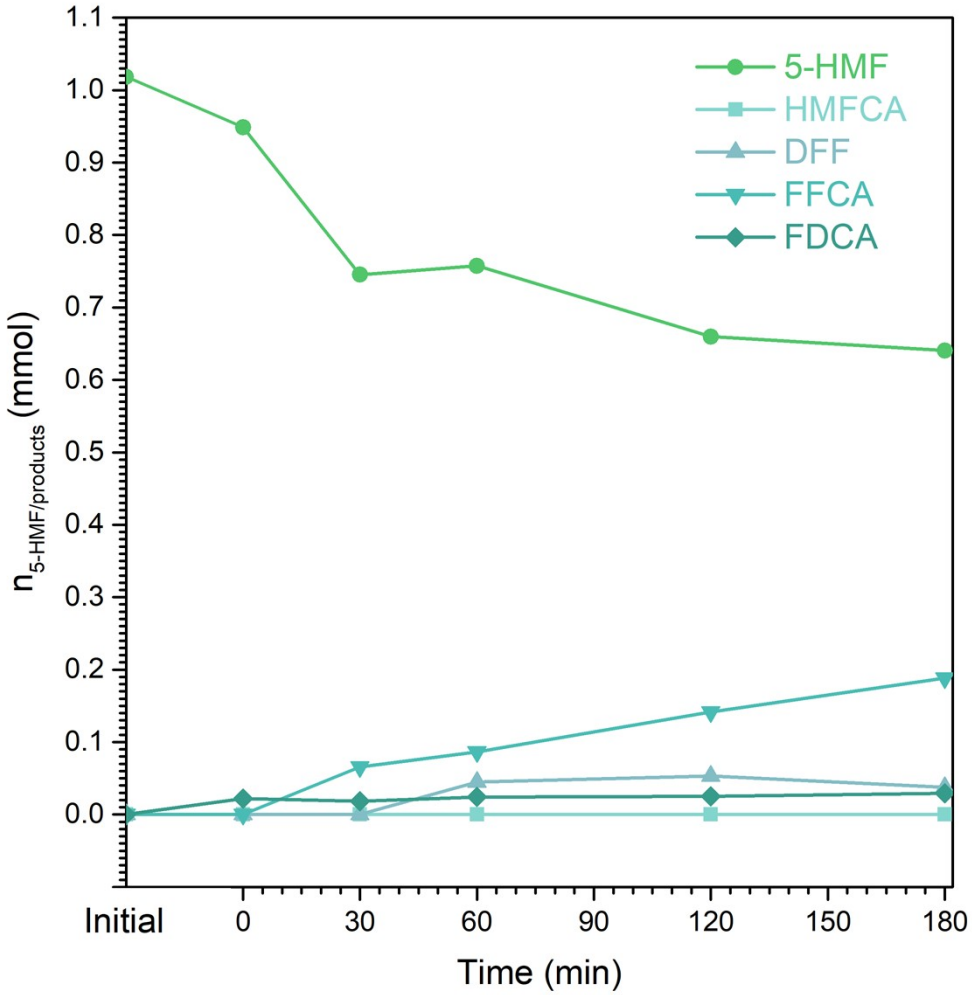

Figure S18. Concentration profiles of 5-HMF and the possible 5-HMF oxidation products (HMFCA, DFF, FFCA, FDCA) measured throughout 3 hours of chronoamperometry with Ni_3B-NCs@CP (0.05 mg/cm^2) at 1.8 V vs RHE in 0.1 M KOH (pH 12.9).

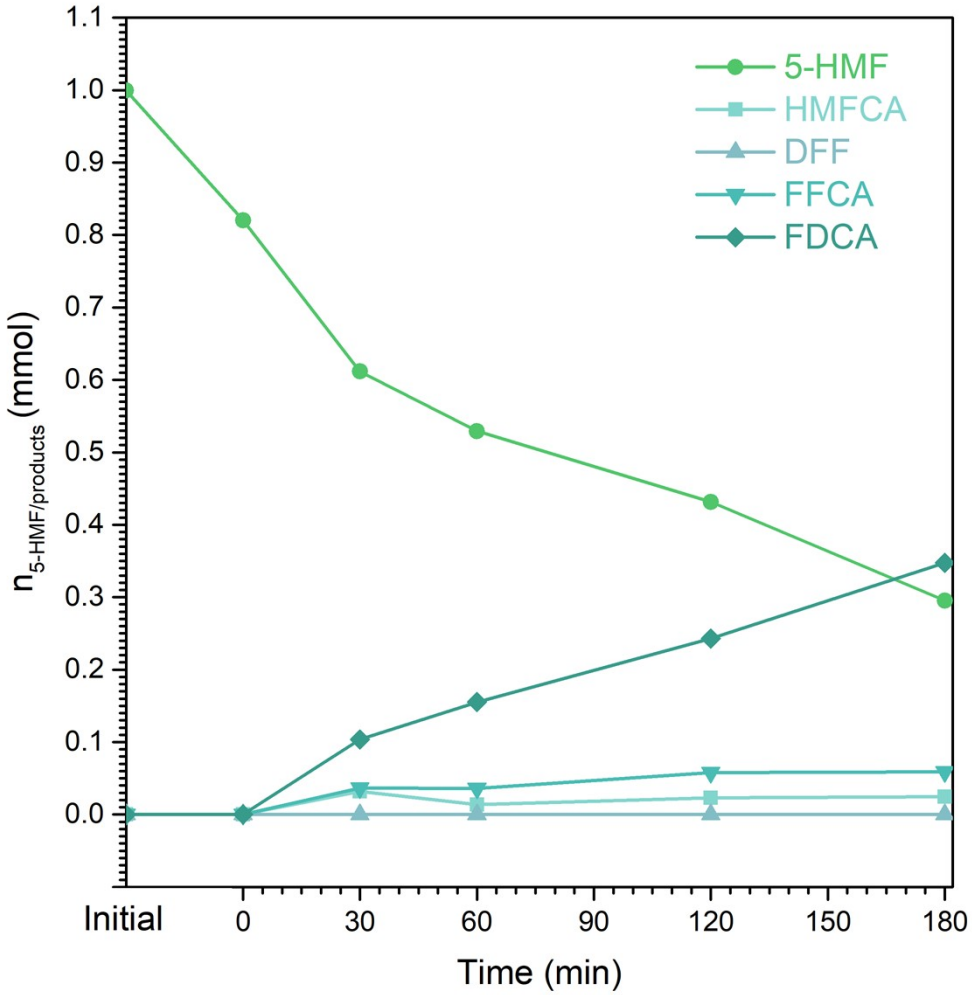

Figure S19. Concentration profiles of 5-HMF and the possible 5-HMF oxidation products (HMFCA, DFF, FFCA, FDCA) measured throughout 3 hours of chronoamperometry with Ni_3B-NCs@CP (0.05 mg/cm^2) at 1.8 V vs RHE in 1 M KOH (pH 13.9).

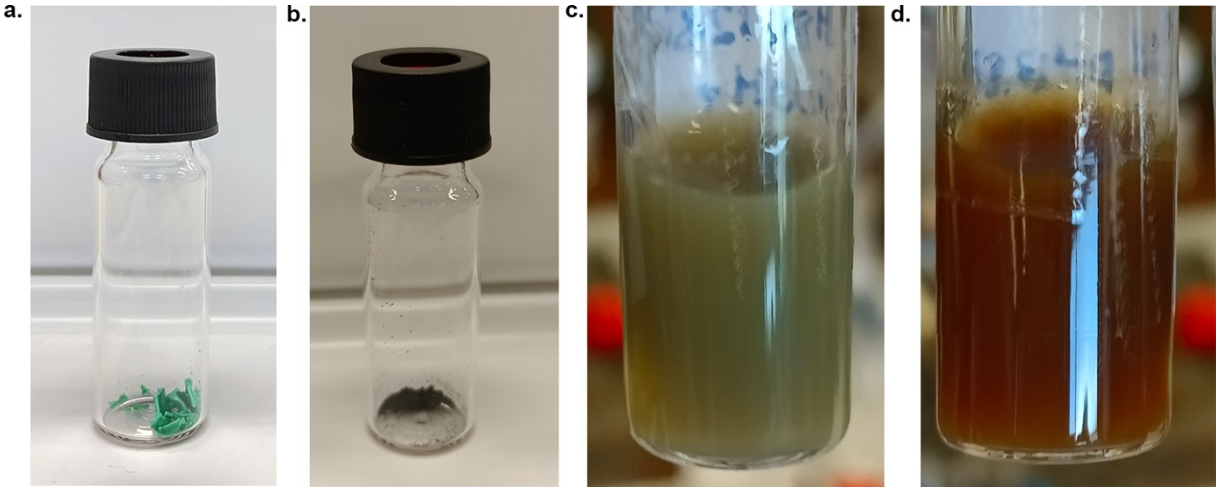

Figure S20. Images of (a) synthesized $Ni(OH)_2$ powder; (b) NiOOH powder; (c) NiOOH mixed with 5-HMF in 0.1 M KOH; (d) NiOOH mixed with 5-HMF in 1 M KOH.

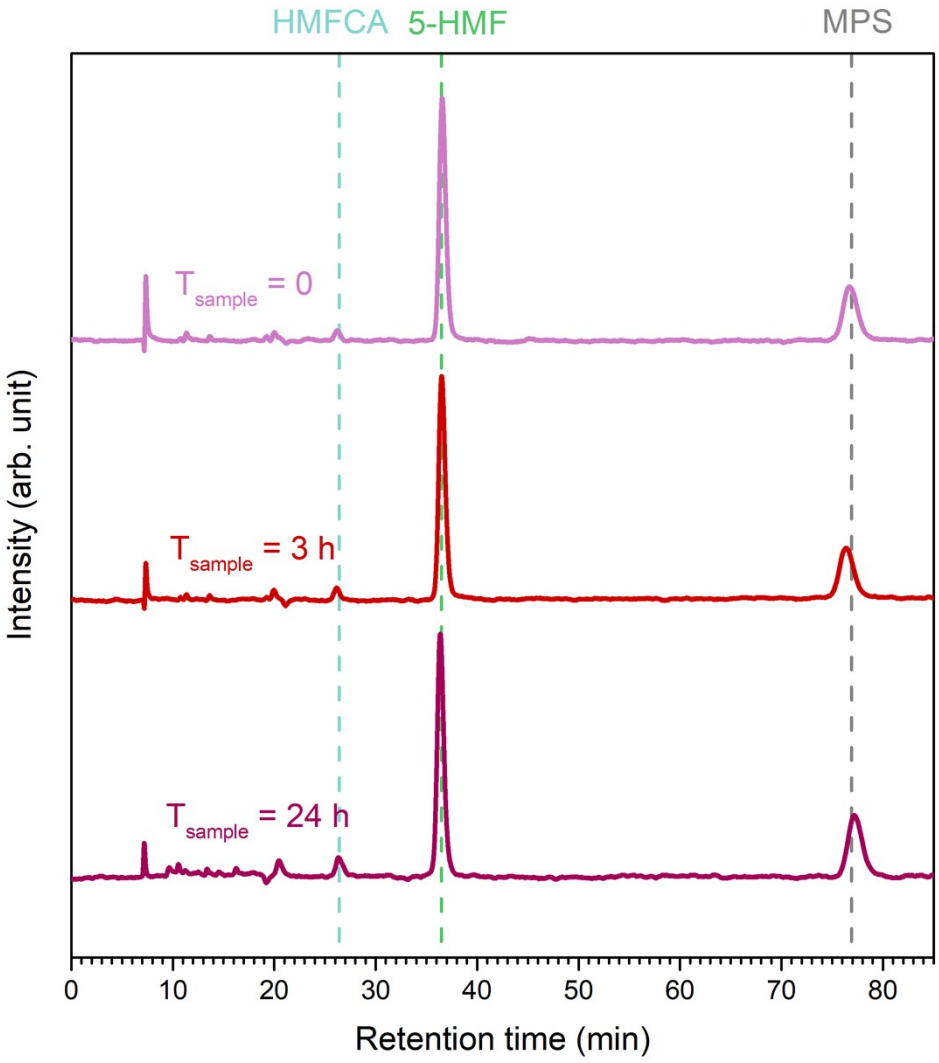

Figure S21. High performance liquid chromatographs (HPLC) analysis recorded by immersing NiOOH in a 5-HMF-containing 0.1 M KOH (pH 12.9) without applying potential. Equimolar amounts of NiOOH and 5-HMF were mixed in 0.1 M KOH and stirred at room temperature. Samples were collected at different times for product analysis. Methyl phenyl sulfone (MPS) was added as internal standard.

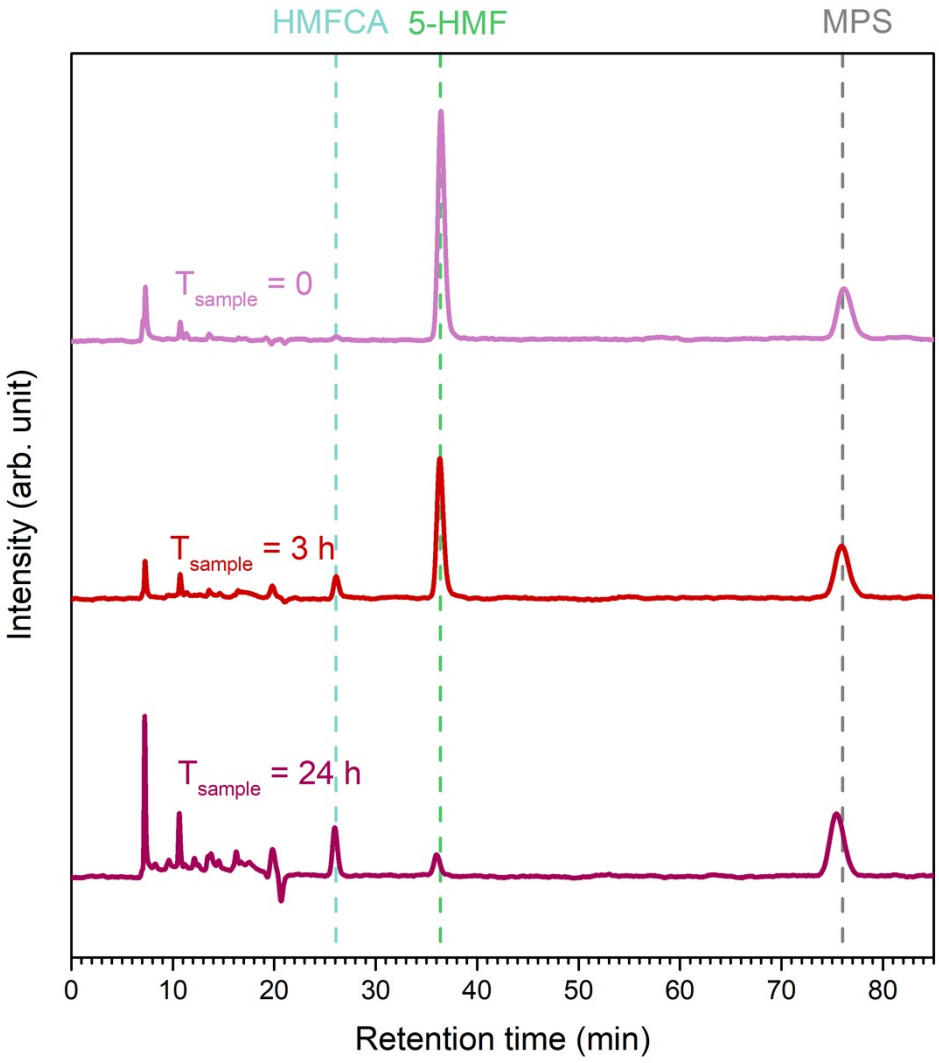

Figure S22. High performance liquid chromatographs (HPLC) analysis recorded by immersing NiOOH in a 5-HMF-containing 0.1 M KOH (pH 12.9) without applying potential. Equimolar amounts of NiOOH and 5-HMF were mixed in 0.1 M KOH and stirred at room temperature. Samples were collected at different times for product analysis. Methyl phenyl sulfone (MPS) was added as internal standard.

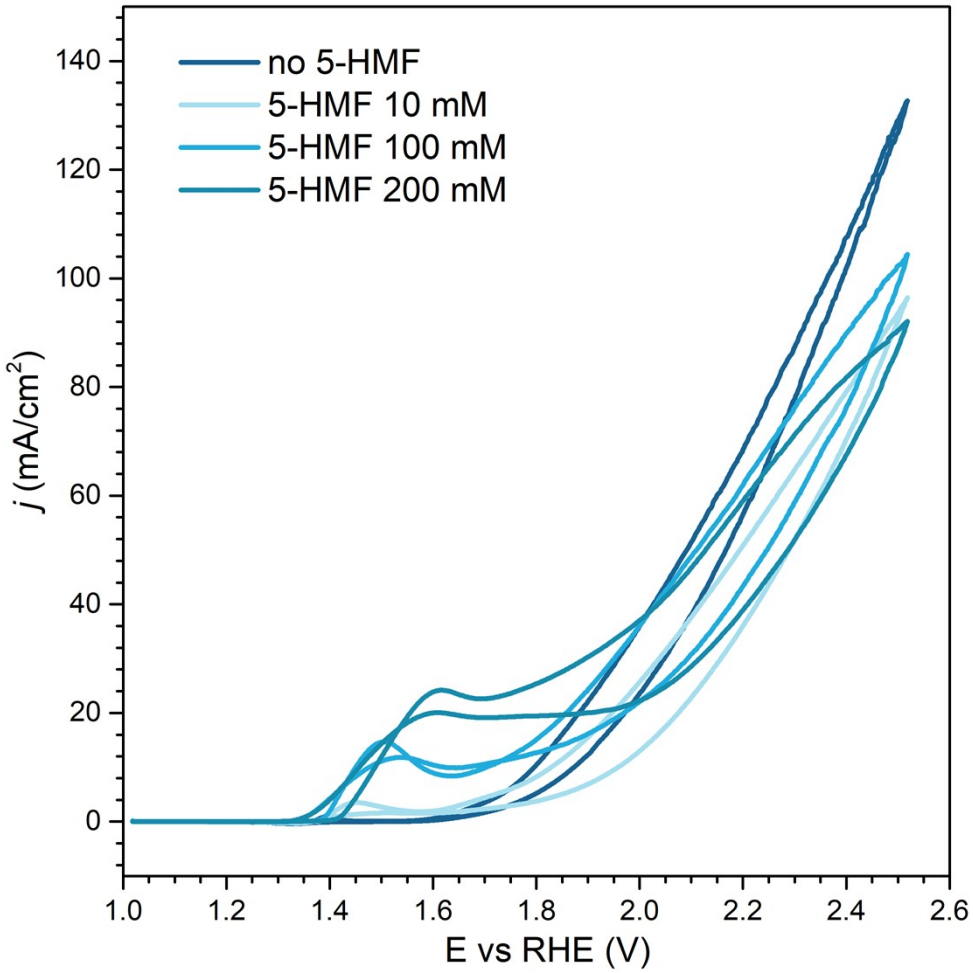

Figure S23. Cyclic voltammetry recorded with scan rate of 10 mV/S for Ni_3B-NCs@CP (0.05 mg/cm^2) measured in 1.0 M KOH (pH 13.9) in the presence of different concentration of 5-HMF (10, 100, 200 mM).

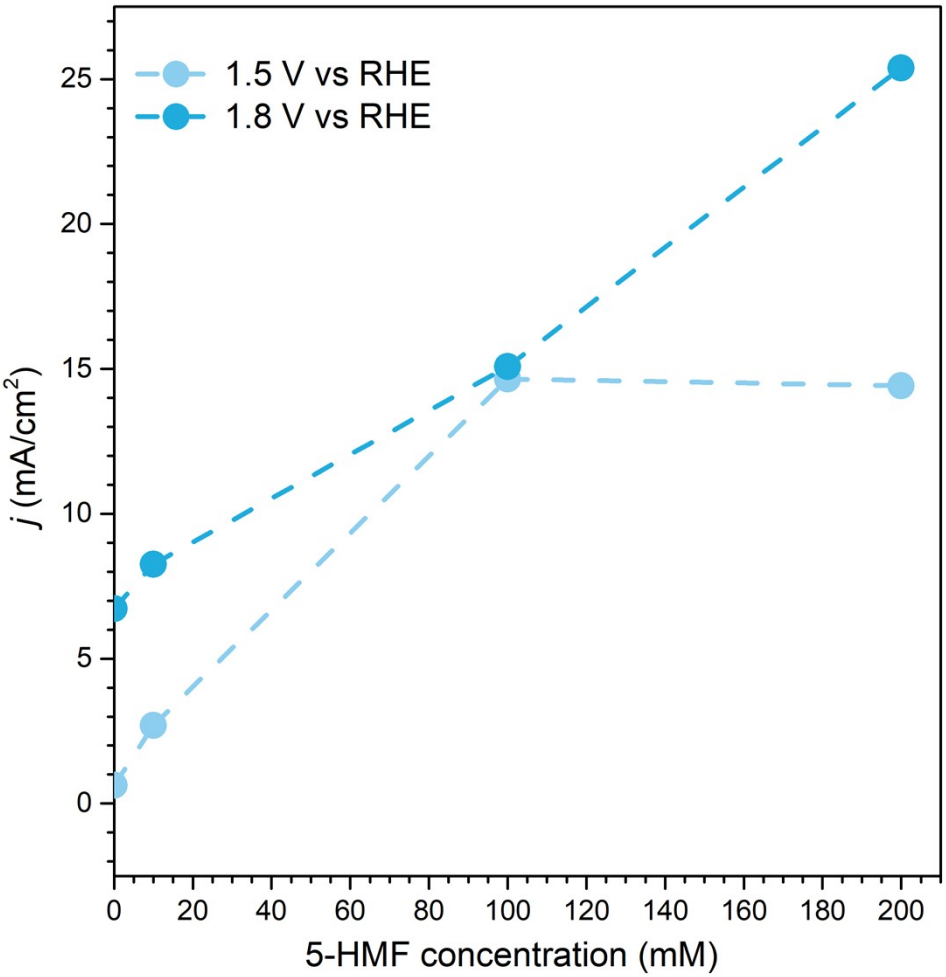

Figure S24. Effect of 5-HMF concentration in the electrolyte (1.0 M KOH) to the current density measured at two potentials (1.5 V vs RHE and 1.8 V vs RHE). The working electrode in this study was Ni_3B-NCs@CP with catalyst loading 0.05 mg/cm^2. The data points plotted in this graph were collected from cyclic voltammogram measured at a scan rate of 10 mV/s.

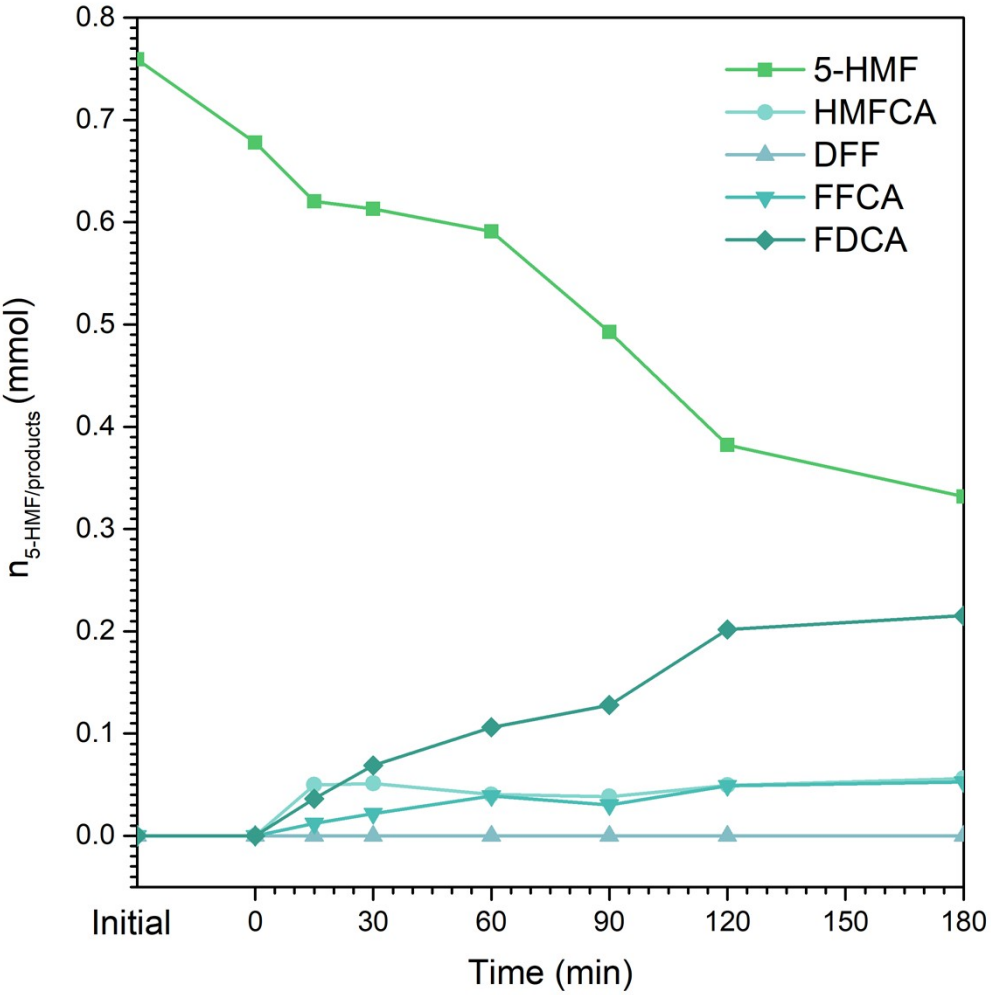

Figure S25. Concentration profiles of 5-HMF and the possible 5-HMF oxidation products (HMFCA, DFF, FFCA, FDCA) measured throughout 3 hours of chronoamperometry with Ni_3B-NCs@CP (0.05 mg/cm^2) at 1.5 V vs RHE in 1 M KOH (pH 13.9).

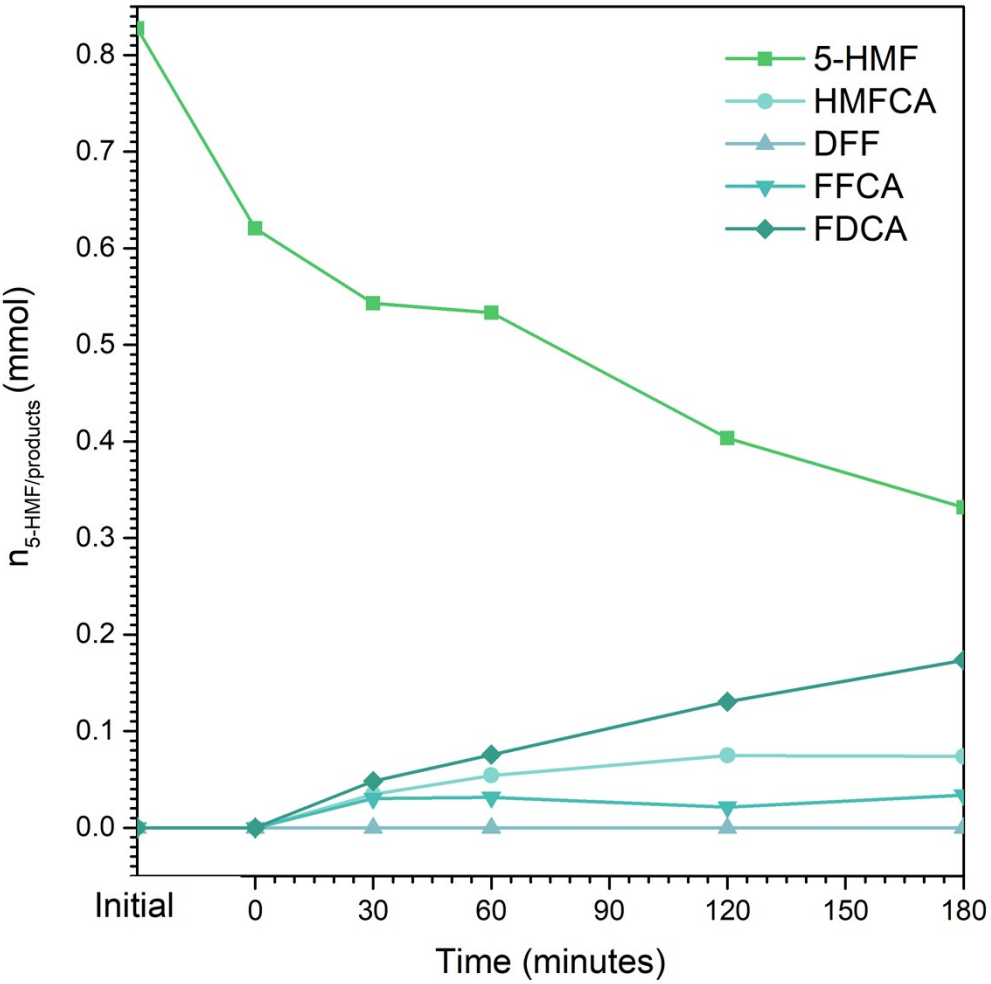

Figure S26. Concentration profiles of 5-HMF and the possible 5-HMF oxidation products (HMFCA, DFF, FFCA, FDCA) measured throughout 3 hours of chronoamperometry with Ni_3B-NCs@CP (0.05 mg/cm^2) at 1.6 V vs RHE in 1 M KOH (pH 13.9).

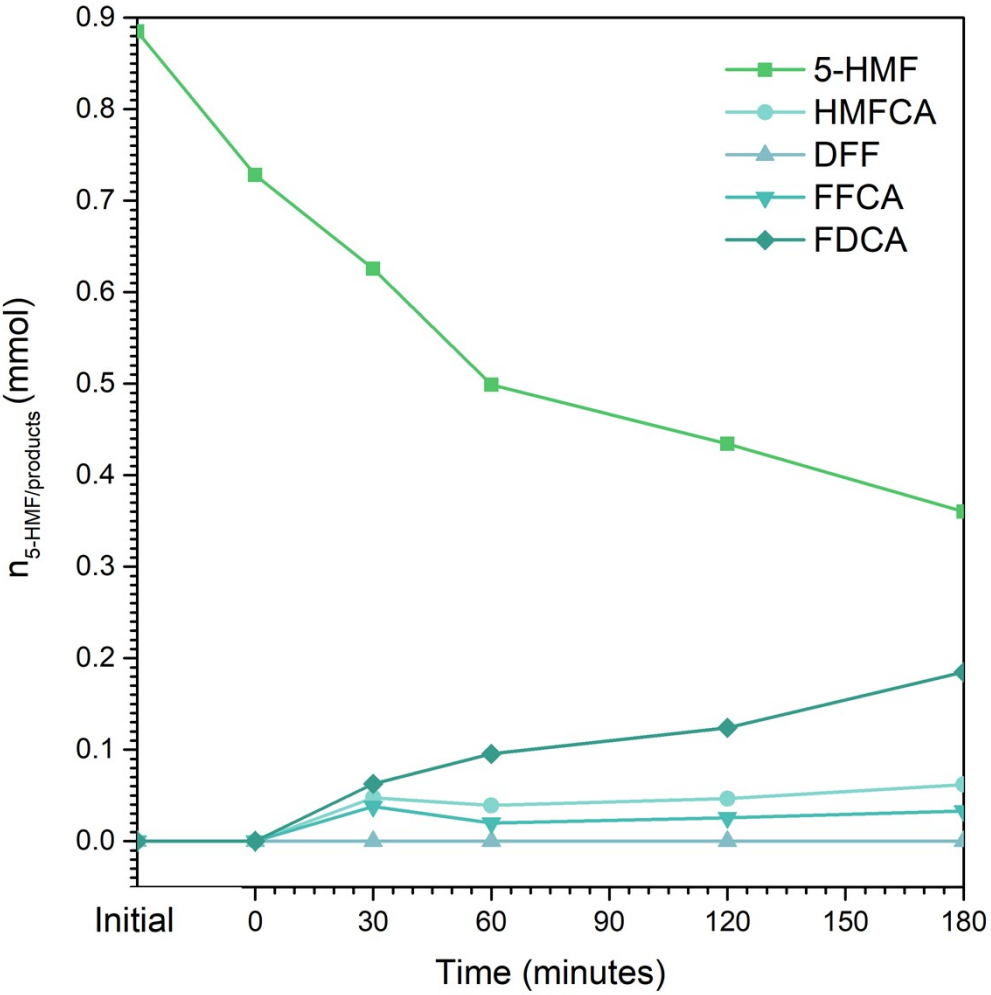

Figure S27. Concentration profiles of 5-HMF and the possible 5-HMF oxidation products (HMFCA, DFF, FFCA, FDCA) measured throughout 3 hours of chronoamperometry with Ni_3B-NCs@CP (0.05 mg/cm^2) at 1.7 V vs RHE in 1 M KOH (pH 13.9).

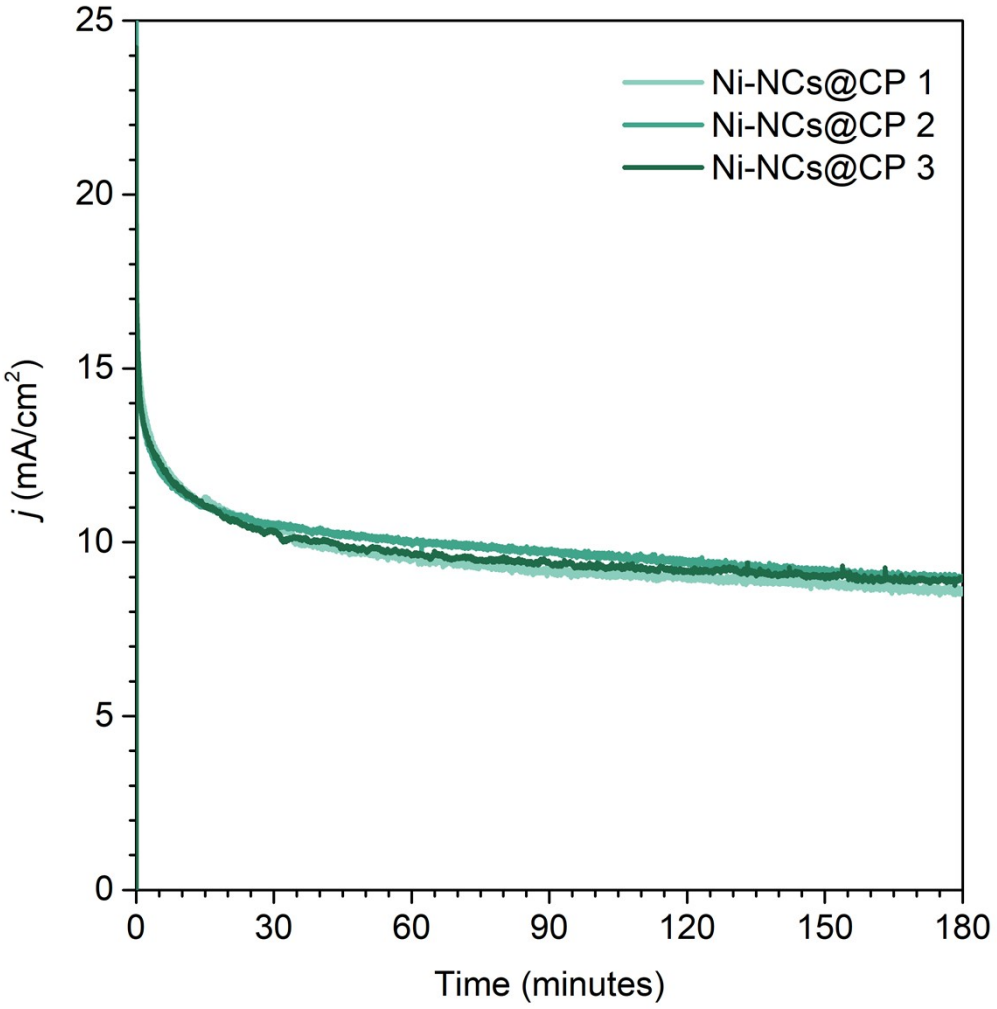

Figure S28. Three independent chronoamperometry of Ni-NCs@CP (0.05 mg/cm^2) conducted at constant potential 1.8 V vs RHE for 3 hours in the presence of 5-HMF (100 mM) at pH 13.9.

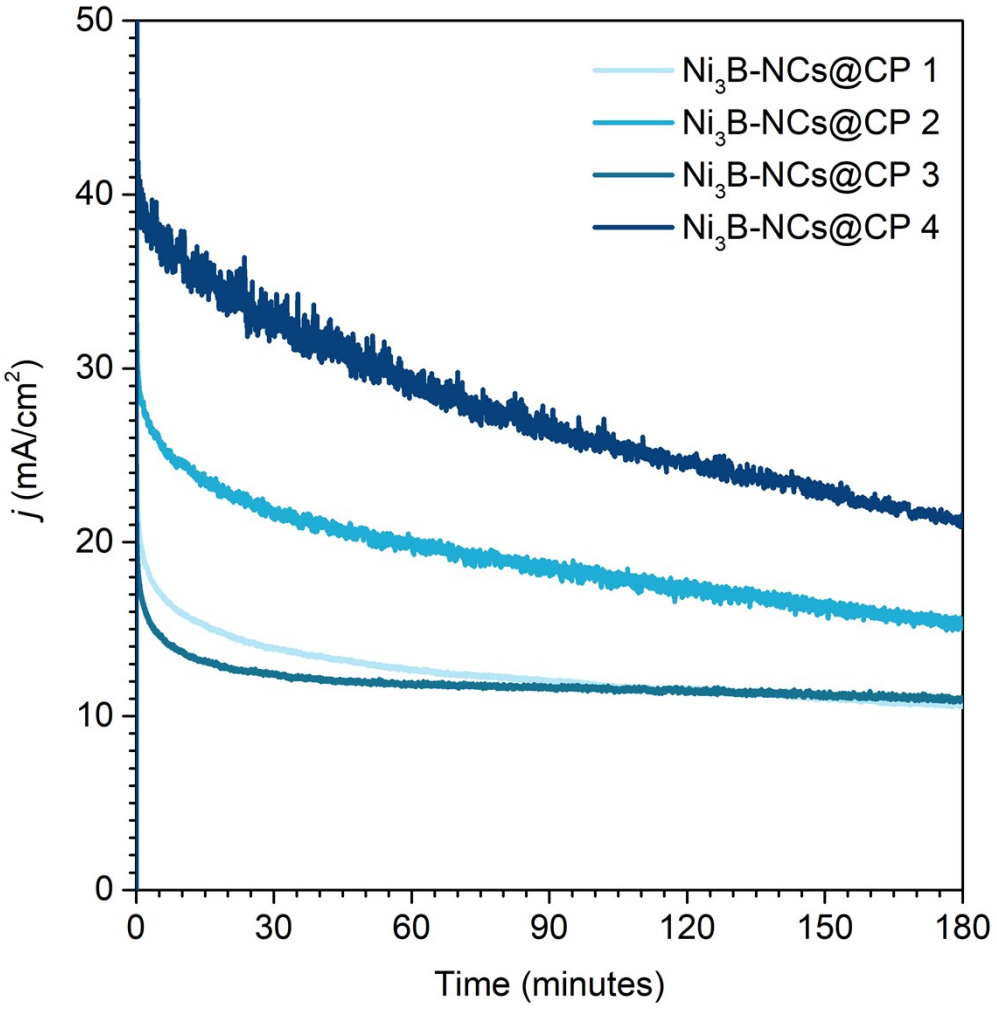

Figure S29. Three independent chronoamperometry of Ni_3B-NCs@CP (0.05 mg/cm^2) conducted at constant potential 1.8 V vs RHE for 3 hours in the presence of 5-HMF (100 mM) at pH 13.9.

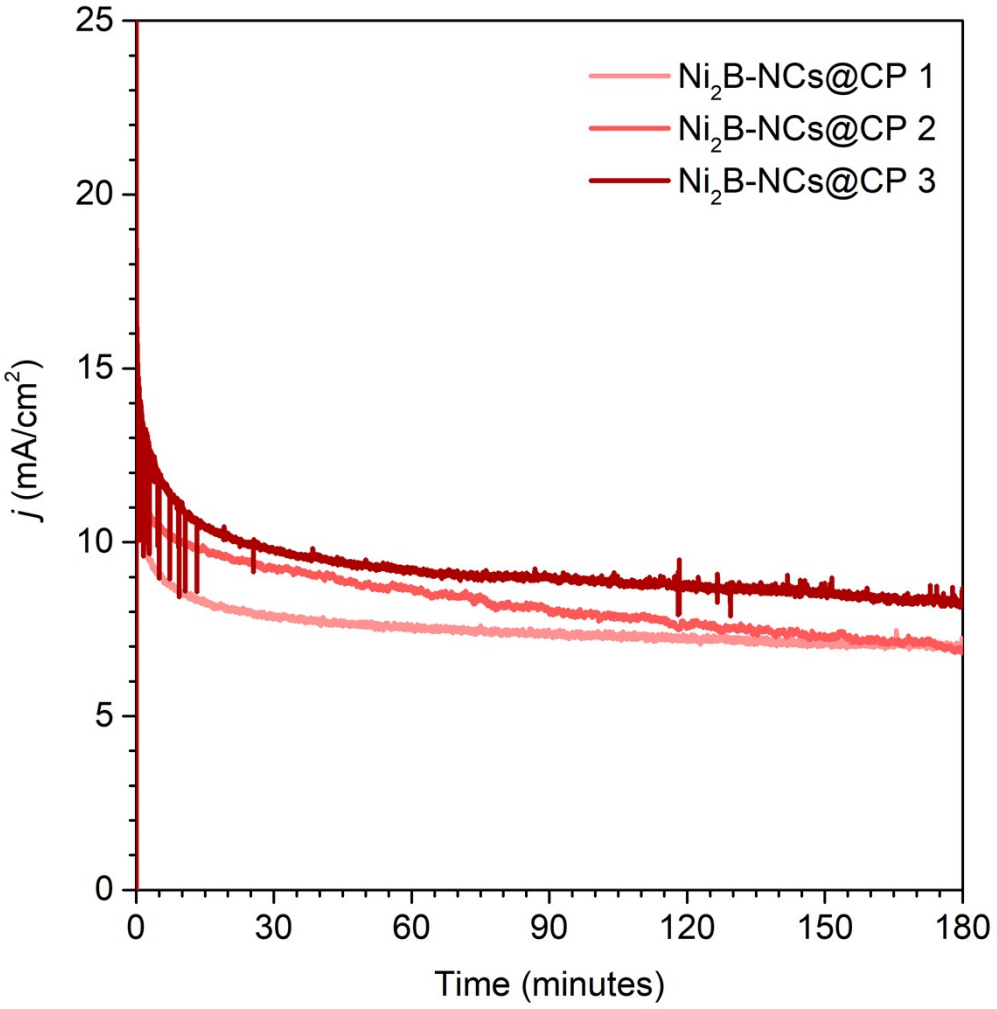

Figure S30. Three independent chronoamperometry of Ni_2B-NCs@CP (0.05 mg/cm^2) conducted at constant potential 1.8 V vs RHE for 3 hours in the presence of 5-HMF (100 mM) at pH 13.9.

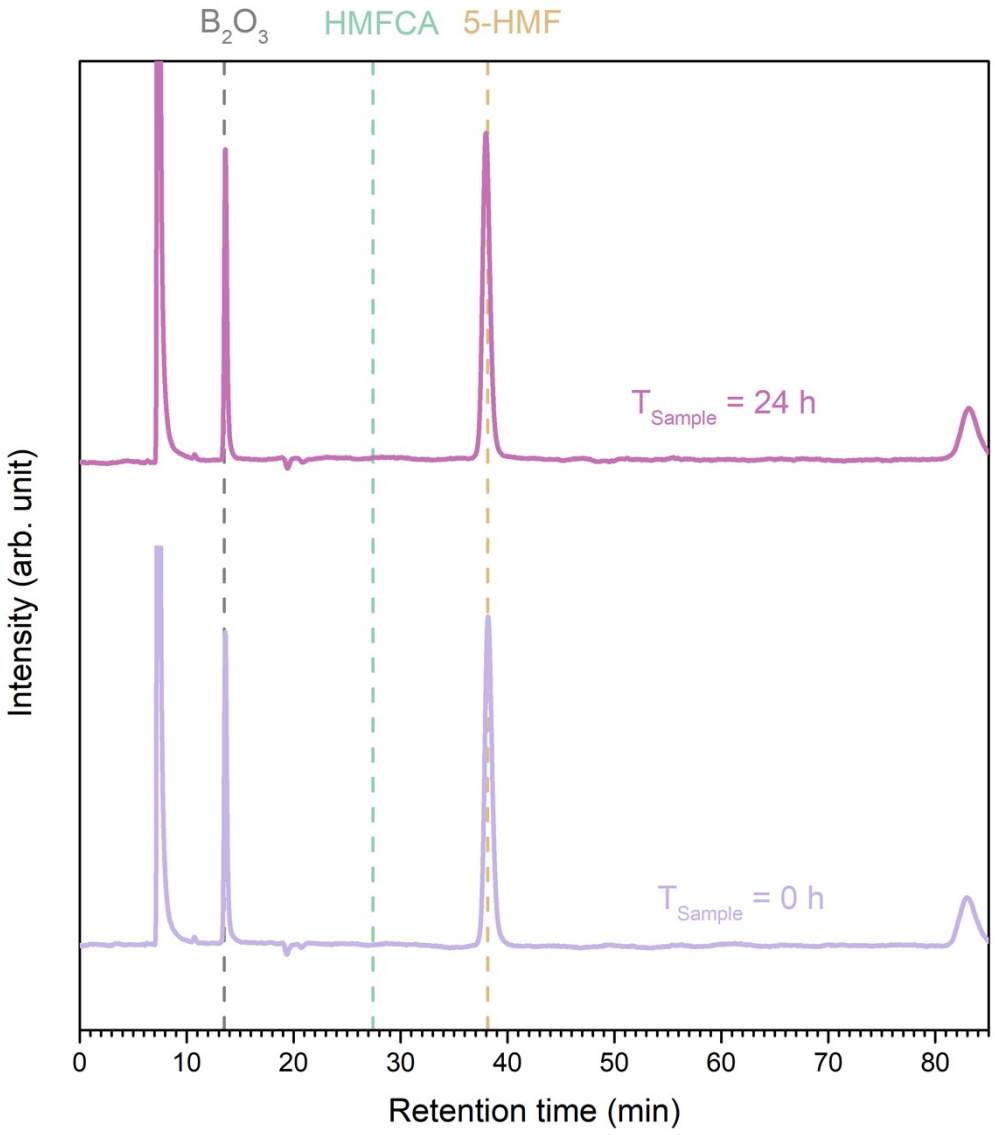

Figure S31. High performance liquid chromatographs (HPLC) analysis recorded by immersing B_2O_3 in a 5-HMF-containing 0.1 M KOH (pH 12.9) without applying potential. Equimolar amounts of $B_2O_3$and 5-HMF were mixed in 0.1 M KOH and stirred at room temperature. Samples were collected at different times for product analysis. Methyl phenyl sulfone (MPS) was added as internal standard.

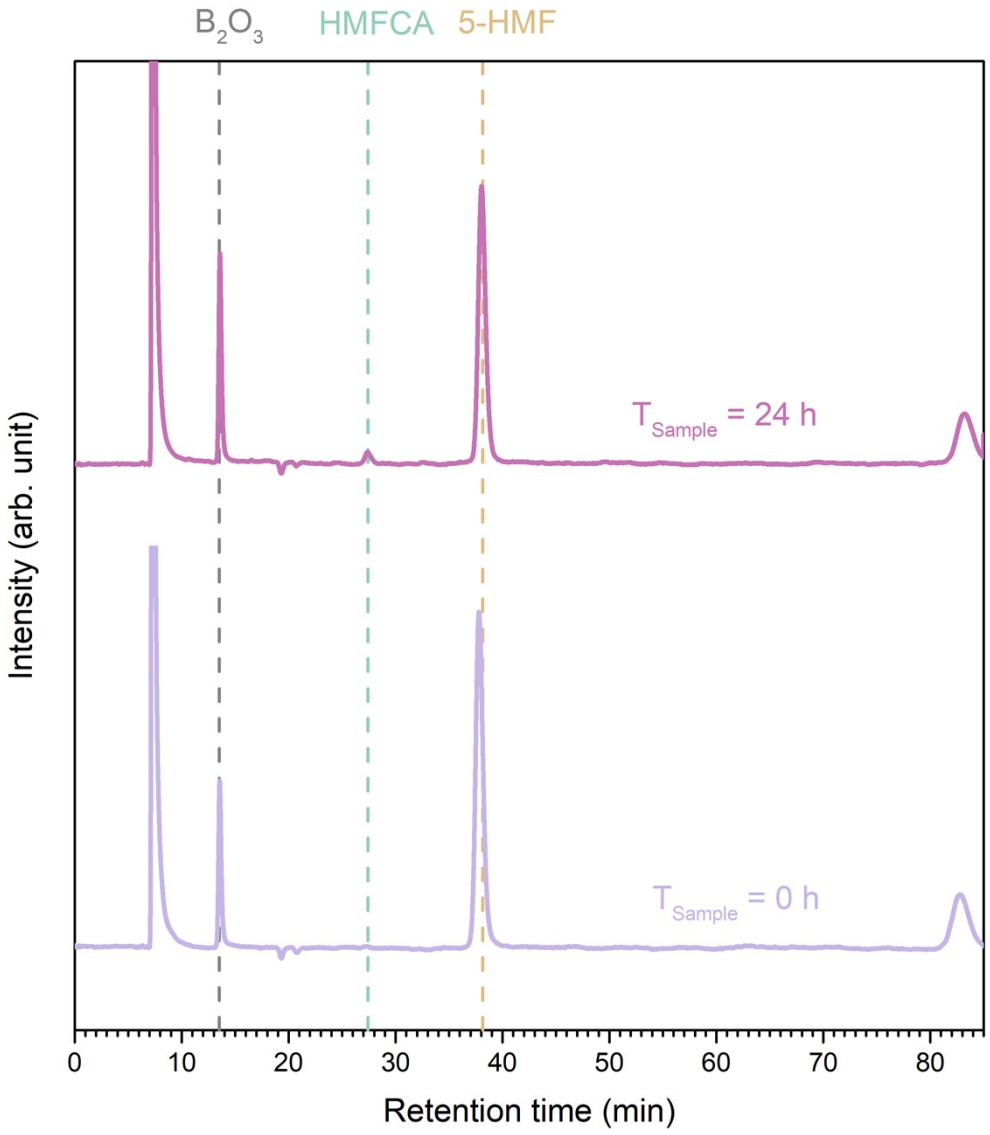

Figure S32. High performance liquid chromatographs (HPLC) analysis recorded by immersing B_2O_3 in a 5-HMF-containing 0.1 M KOH (pH 13.9) without applying potential. Equimolar amounts of $B_2O_3$and 5-HMF were mixed in 1 M KOH and stirred at room temperature. Samples were collected at different times for product analysis. Methyl phenyl sulfone (MPS) was added as internal standard.

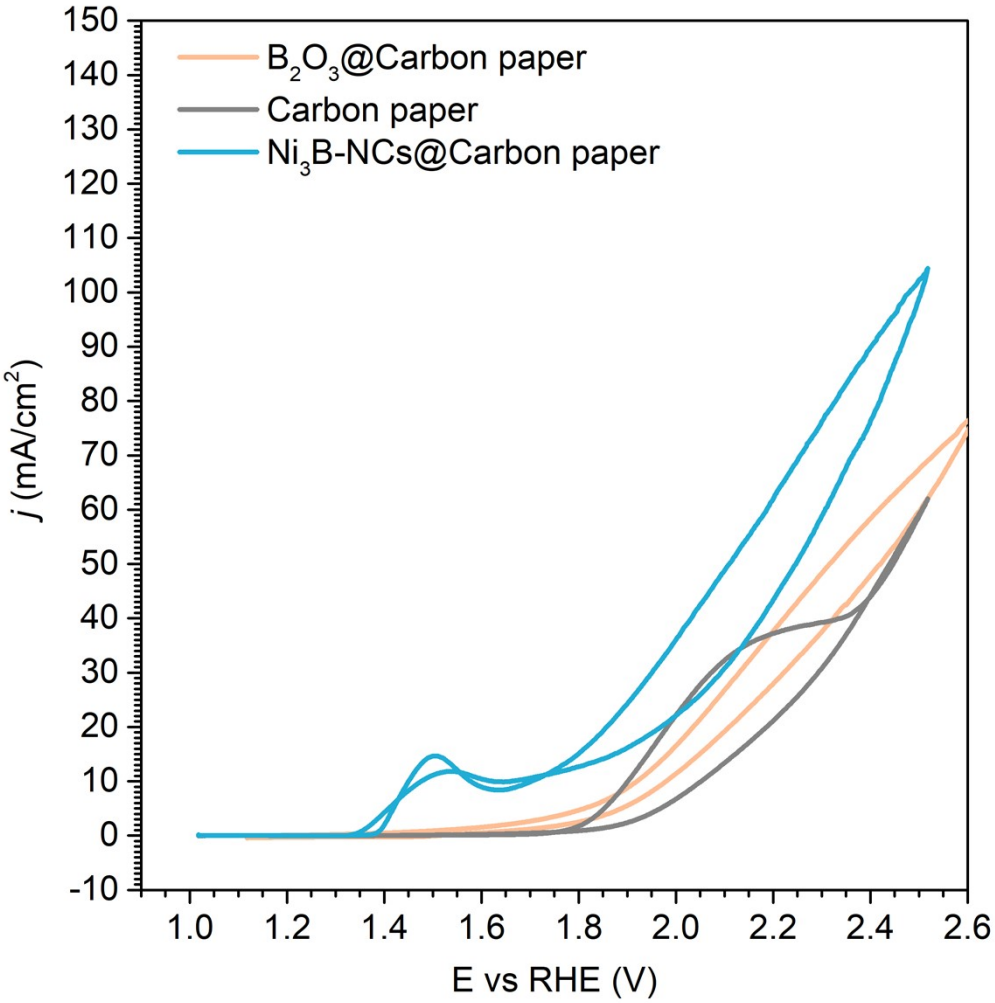

Figure S33. Cyclic voltammetry recorded with scan rate of 10 mV/S for B_2O_3@CP (1 mg/cm^2), carbon paper, and Ni_3B-NCs@CP (0.05 mg/cm^2) measured in 1.0 M KOH (pH 13.9) in the presence of 100 mM 5-HMF.

Recycling tests

The figures below (S34-S38) present the chronoamperometries and the reactants concentration profiles for the recycling tests of the Ni_3B-NCs@CP electrocatalyst. It is worth noting that higher initial current densities (but also higher level of noise) were observed the second and third run of the electrode recyclability tests, most likely due to the higher environmental temperature during those experiments, which also resulted in higher 5-HMF conversion.

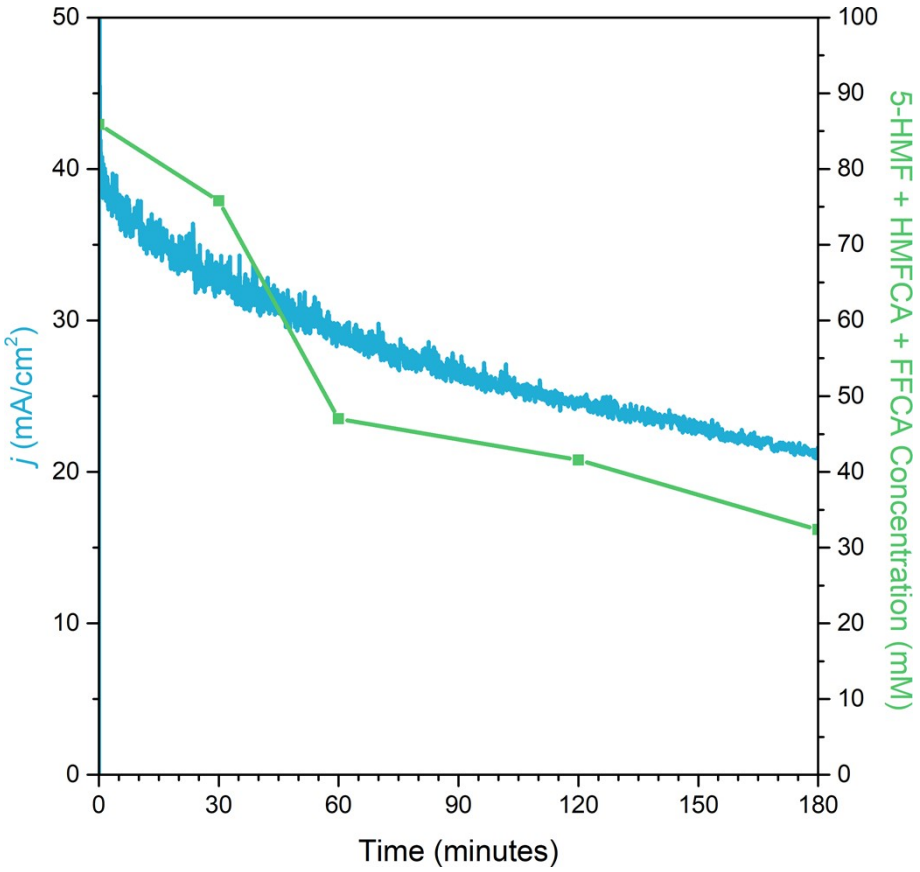

Figure S34. 1st chronoamperometric run of Ni_3B-NCs@CP conducted at constant potential 1.8 V vs RHE for 3 hours showing current density and the sum of 5-HMF, HMFCA, and FFCA concentrations as a function of time.

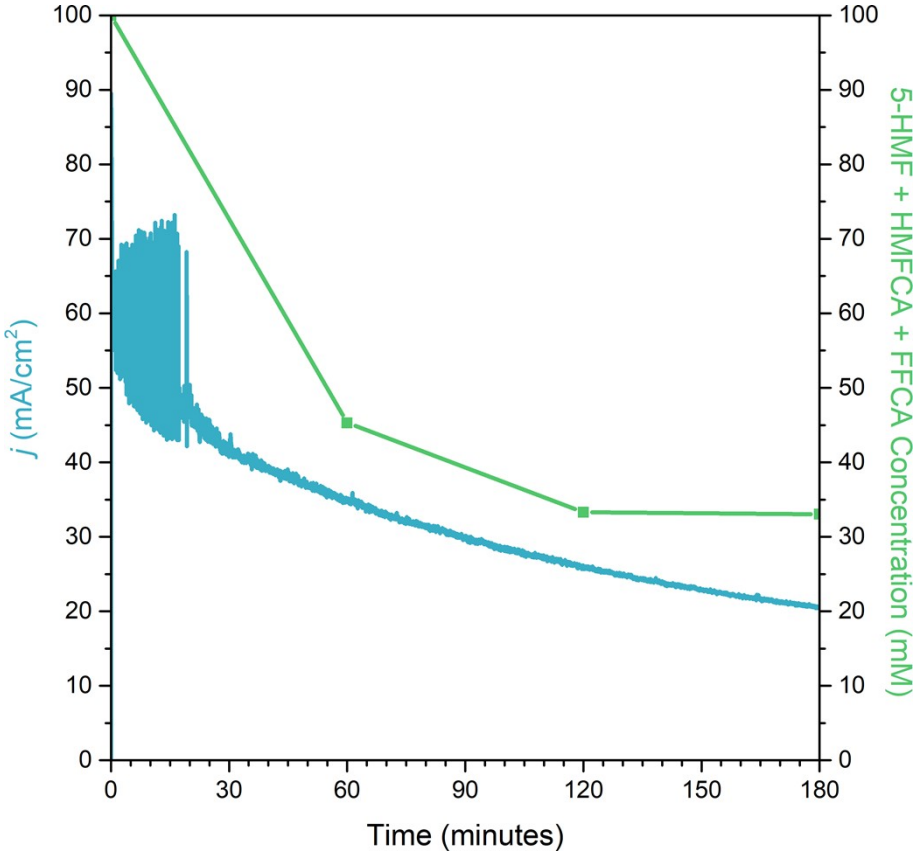

Figure S35. 2nd chronoamperometric run of Ni_3B-NCs@CP conducted at constant potential 1.8 V vs RHE for 3 hours showing current density and the sum of 5-HMF, HMFCA, and FFCA concentrations as a function of time.

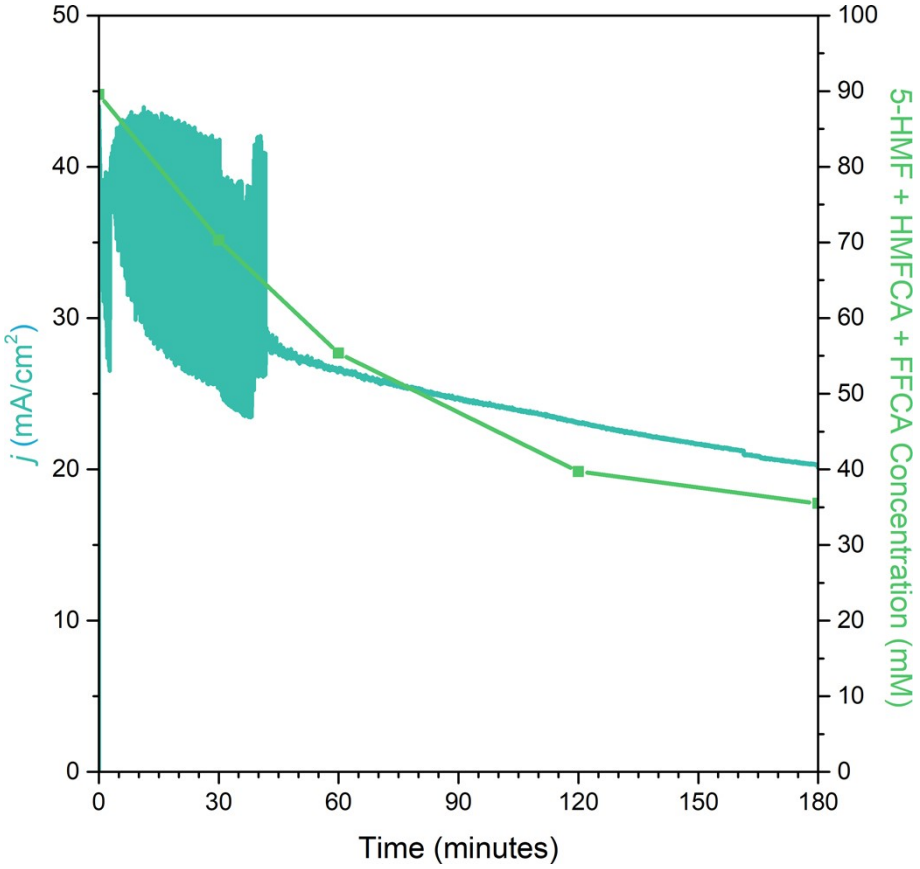

Figure S36. 3rd chronoamperometric run of Ni_3B-NCs@CP conducted at constant potential 1.8 V vs RHE for 3 hours showing current density and the sum of 5-HMF, HMFCA, and FFCA concentrations as a function of time.

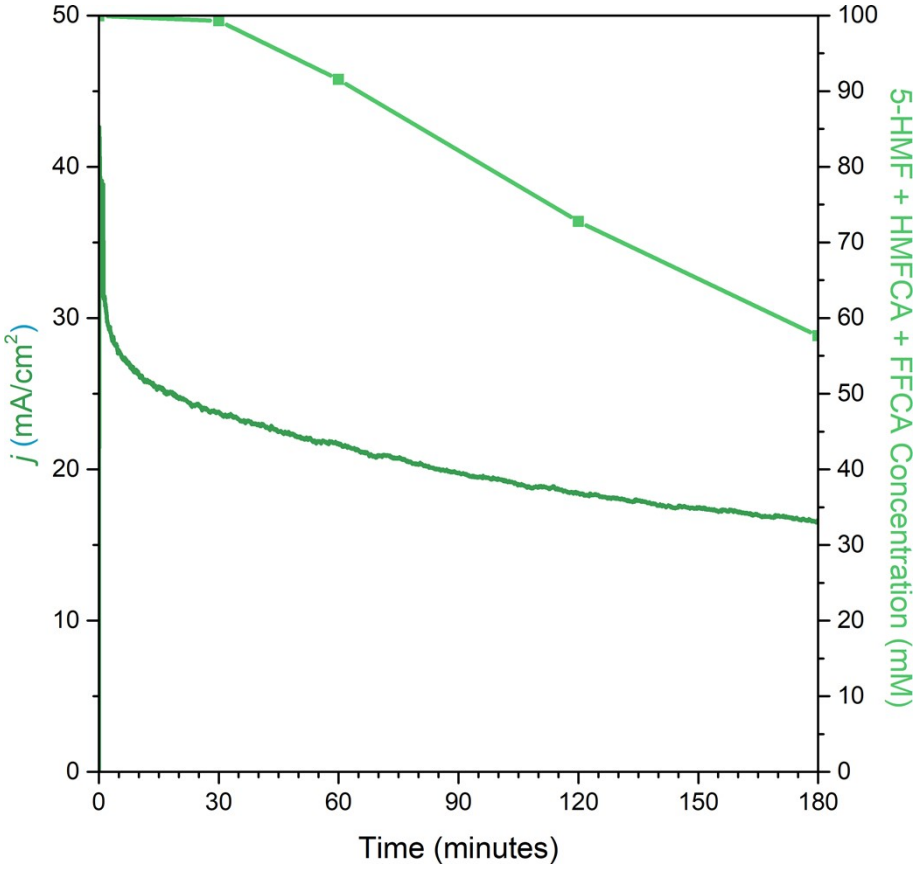

Figure S37. 4th chronoamperometric run of Ni_3B-NCs@CP conducted at constant potential 1.8 V vs RHE for 3 hours showing current density and the sum of 5-HMF, HMFCA, and FFCA concentrations as a function of time.

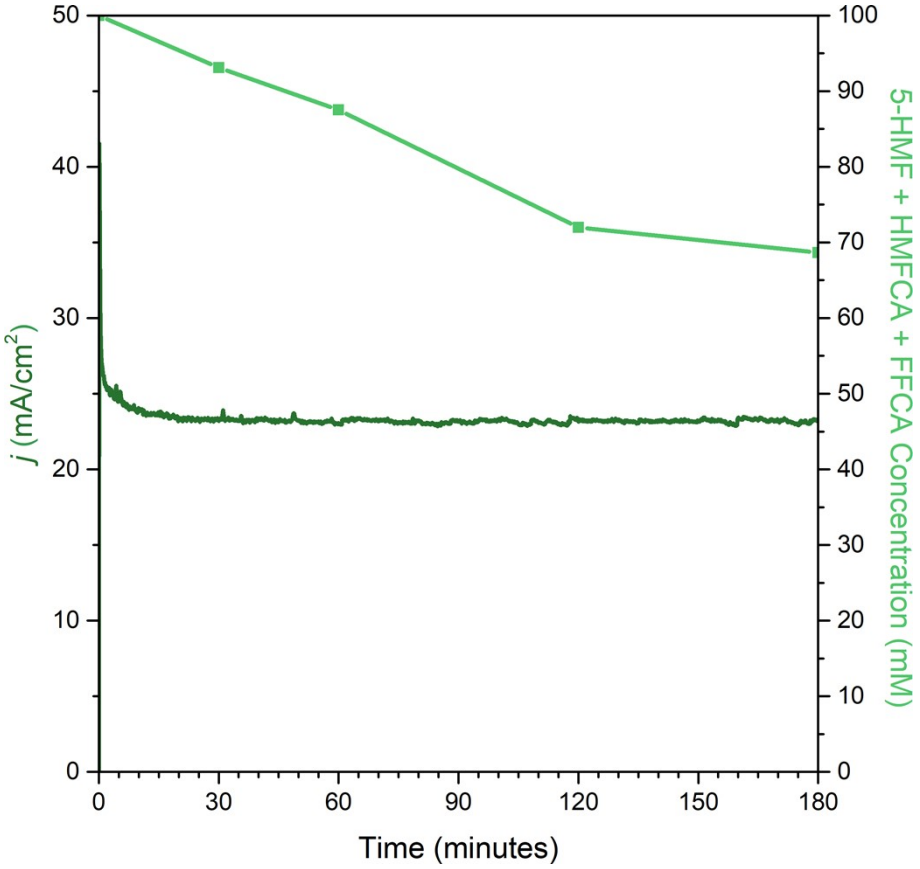

Figure S38. 5th chronoamperometric run of Ni_3B-NCs@CP conducted at constant potential 1.8 V vs RHE for 3 hours showing current density and the sum of 5-HMF, HMFCA, and FFCA concentrations as a function of time.

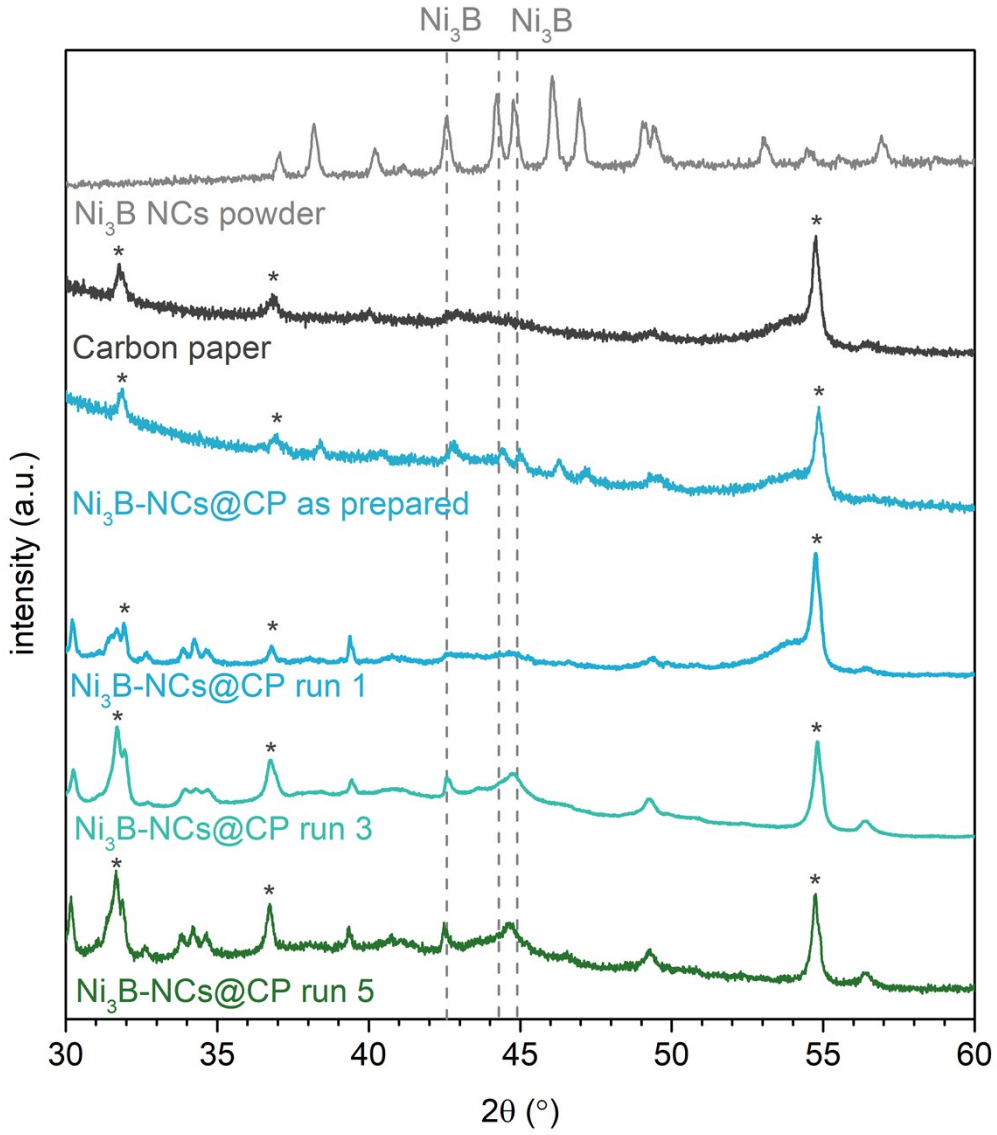

Figure S39. XRD patterns of Ni_3B-NCs@CP as prepared, and after the first, third and fifth runs of electrooxidation of 5-HMF at pH 13.9 at 1.8 V vs RHE for 3 hours. XRD of the carbon paper and Ni_3B NCs have also been plotted as references.

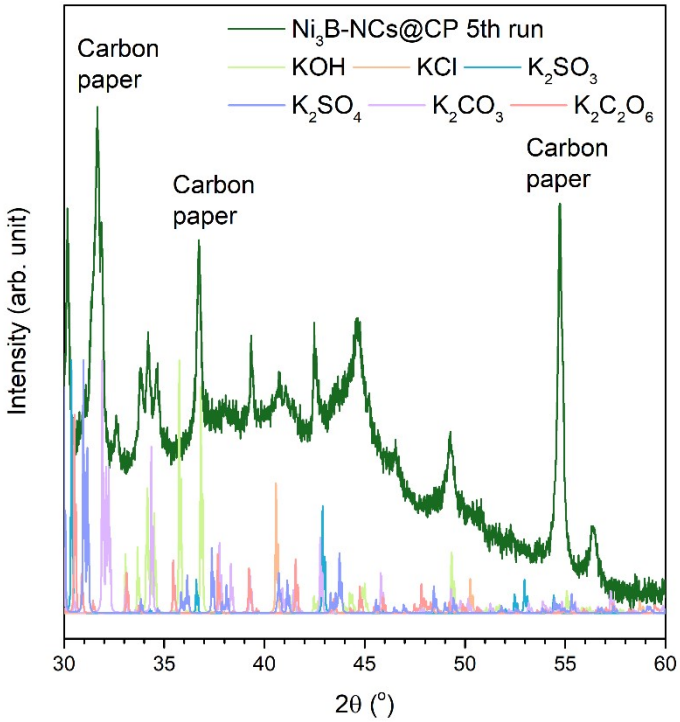

Figure S40. XRD patterns of Ni_3B-NCs@CP after the fifth run of electrooxidation of 5-HMF at pH 13.9 at 1.8 V vs RHE for 3 h.

The lower angle peaks emerging after the electrochemical tests have been identified as KOH, KCl, K_2CO_3, $K_2C_2O_6$, K_2SO_3 and K_2SO_4. KOH originates from the electrolyte, whereas the other salts may stem from the reaction between K^+ in the electrolyte and other species present as impurities (e.g. Cl^-, which is present on the Ni_3B surface, as shown by XPS) or generated during the reaction (e.g. carbonate and oxalate anions formed by the oxidative degradation of carbon paper; sulphates and sulphites coming from Nafion).

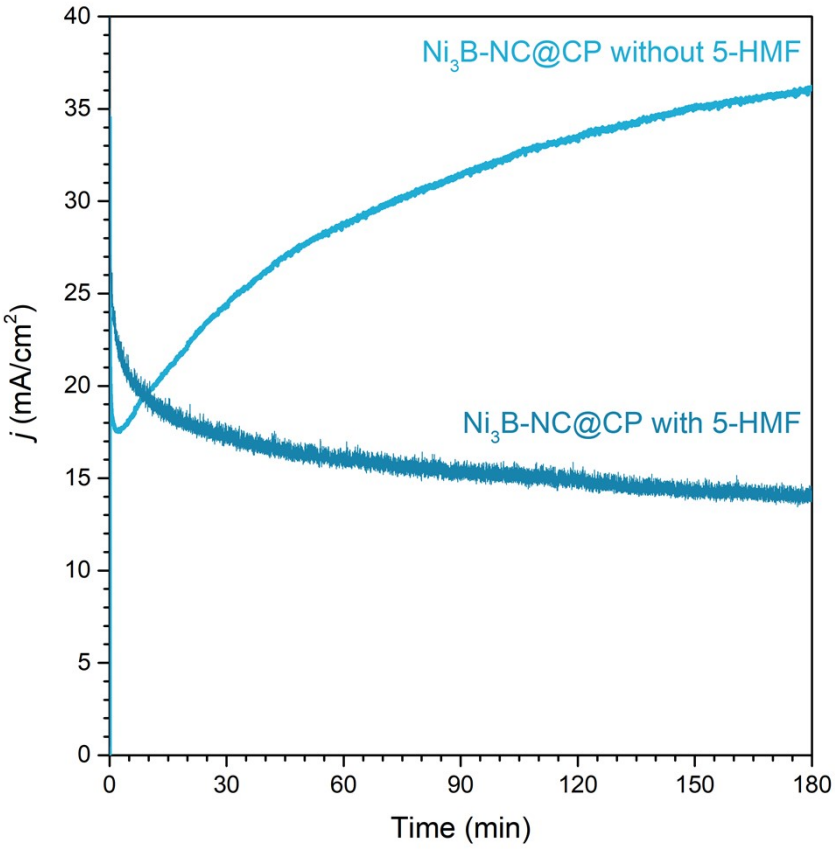

Figure S41. Chronoamperometry of Ni_3B-NCs@CP with catalyst loading 0.05 mg/cm^2 in 1 M KOH (pH 13.9) at 1.8 V vs RHE with 100 mM of 5-HMF and no 5-HMF.

The fact that the chronoamperometry of Ni_3B-NCs@CP at 1.8 V vs RHE in the absence of 5-HMF and at pH 13.9 shows a trend of increasing current density suggests that besides the OER, under these conditions significant oxidation of the electrode is taking place, most likely as a consequence of gradual oxidative degradation of the carbon paper support. It is worth noting that this phenomenon seems to be largely suppressed in the presence of 5-HMF, which can be thus considered to be more prone to undergo oxidation than the carbon paper support.

References

1. S. Barwe, J. Weidner, S. Cychy, D. M. Morales, S. Dieckhöfer, D. Hiltrop, J. Masa, M. Muhler and W. Schuhmann, *Angew. Chem. Int. Ed.*, 2018, **57**, 11460-11464.
2. P. Zhang, X. Sheng, X. Chen, Z. Fang, J. Jiang, M. Wang, F. Li, L. Fan, Y. Ren, B. Zhang, B. J. J. Timmer, M. S. G. Ahlquist and L. Sun, *Angew. Chem. Int. Ed.*, 2019, **58**, 9155-9159.
3. X. Song, X. Liu, H. Wang, Y. Guo and Y. Wang, *Ind. Eng. Chem. Res.*, 2020, **59**, 17348-17356.
4. C. Wang, Y. Wu, A. Bodach, M. L. Krebs, W. Schuhmann and F. Schüth, *Angew. Chem. Int. Ed.*, 2023, **62**, e202215804.
5. G. Grabowski, J. Lewkowski and R. Skowroński, *Electrochim. Acta*, 1991, **36**, 1995.
6. B. You, X. Liu, N. Jiang and Y. Sun, *J. Am. Chem. Soc.*, 2016, **138**, 13639-13646.
7. B. You, N. Jiang, X. Liu and Y. Sun, *Angew. Chem., Int. Ed. Engl.*, 2016, **55**, 9913-9917.
8. B. You, X. Liu, X. Liu and Y. Sun, *ACS Catal.*, 2017, **7**, 4564-4570.
9. M. Li, L. Chen, S. Ye, G. Fan, L. Yang, X. Zhang and F. Li, *J. Mater. Chem. A*, 2019, **7**, 13695-13704.
10. A. R. Poerwoprajitno, L. Gloag, J. Watt, S. Cychy, S. Cheong, P. V. Kumar, T. M. Benedetti, C. Deng, K.-H. Wu, C. E. Marjo, D. L. Huber, M. Muhler, J. J. Gooding, W. Schuhmann, D.-W. Wang and R. D. Tilley, *Angew. Chem. Int. Ed.*, 2020, **59**, 15487-15491.
11. N. Zhang, Y. Zou, L. Tao, W. Chen, L. Zhou, Z. Liu, B. Zhou, G. Huang, H. Lin and S. Wang, *Angew. Chem. Int. Ed.*, 2019, **58**, 15895-15903.
12. Y. Lu, C.-L. Dong, Y.-C. Huang, Y. Zou, Y. Liu, Y. Li, N. Zhang, W. Chen, L. Zhou, H. Lin and S. Wang, *Sci. China Chem.*, 2020, **63**, 980-986.
13. X. Chen, X. Zhong, B. Yuan, S. Li, Y. Gu, Q. Zhang, G. Zhuang, X. Li, S. Deng and J.-g. Wang, *Green Chem.*, 2019, **21**, 578-588.
14. X. Deng, M. Li, Y. Fan, L. Wang, X.-Z. Fu and J.-L. Luo, *Appl. Catal. B Environ.*, 2020, **278**, 119339.
15. L. Gao, Z. Liu, J. Ma, L. Zhong, Z. Song, J. Xu, S. Gan, D. Han and L. Niu, *Appl. Catal. B Environ.*, 2020, **261**, 118235.
16. S. Choi, M. Balamurugan, K.-G. Lee, K. H. Cho, S. Park, H. Seo and K. T. Nam, *J. Phys. Chem. Lett.*, 2020, **11**, 2941-2948.
17. N. Heidary and N. Kornienko, *ChemComm*, 2019, **55**, 11996-11999.
18. B. J. Taitt, D.-H. Nam and K.-S. Choi, *ACS Catal.*, 2019, **9**, 660-670.
19. M. Cai, Y. Zhang, Y. Zhao, Q. Liu, Y. Li and G. Li, *J. Mater. Chem. A*, 2020, **8**, 20386-20392.
20. W. Chen, C. Xie, Y. Wang, Y. Zou, C.-L. Dong, Y.-C. Huang, Z. Xiao, Z. Wei, S. Du, C. Chen, B. Zhou, J. Ma and S. Wang, *Chem*, 2020, **6**, 2974-2993.
21. K. Zhang, Z. Zhan, M. Zhu, H. Lai, X. He, W. Deng, Q. Zhang and Y. Wang, *J. Energy Chem.*, 2023, **80**, 58-67.
22. W.-J. Liu, L. Dang, Z. Xu, H.-Q. Yu, S. Jin and G. W. Huber, *ACS Catal.*, 2018, **8**, 5533-5541.
23. S. Yang, Y. Guo, P. Zhao, H. Jiang, H. Shen, Z. Chen, L. Jiang, X. Xue, Q. Zhang and H. Zhang, *ACS Catal.*, 2024, **14**, 449-462.
24. X. Lu, K.-H. Wu, B. Zhang, J. Chen, F. Li, B.-J. Su, P. Yan, J.-M. Chen and W. Qi, *Angew. Chem. Int. Ed.*, 2021, **60**, 14528-14535.
25. M. Zhang, Y. Liu, B. Liu, Z. Chen, H. Xu and K. Yan, *ACS Catal.*, 2020, **10**, 5179-5189.
26. M. J. Kang, H. Park, J. Jegal, S. Y. Hwang, Y. S. Kang and H. G. Cha, *Appl. Catal. B Environ.*, 2019, **242**, 85-91.
27. Y. Zhong, R.-Q. Ren, J.-B. Wang, Y.-Y. Peng, Q. Li and Y.-M. Fan, *Catal. Sci. Technol.*, 2022, **12**, 201-211.
28. Z. Zhao, T. Guo, X. Luo, X. Qin, L. Zheng, L. Yu, Z. Lv, D. Ma and H. Zheng, *Catal. Sci. Technol.*, 2022, **12**, 3817-3825.
29. Y.-F. Qi, K.-Y. Wang, Y. Sun, J. Wang and C. Wang, *ACS Sustain. Chem. Eng*, 2022, **10**, 645-654.
30. Y. Xie, Z. Zhou, N. Yang and G. Zhao, *Adv. Funct. Mater.*, 2021, **31**, 2102886.

31. L. Gao, X. Wen, S. Liu, D. Qu, Y. Ma, J. Feng, Z. Zhong, H. Guan and L. Niu, *J. Mater. Chem. A*, 2022, **10**, 21135-21141.
32. L. Zheng, Y. Zhao, P. Xu, Z. Lv, X. Shi and H. Zheng, *J. Mater. Chem. A*, 2022, **10**, 10181-10191.
33. R. Ge, Y. Wang, Z. Li, M. Xu, S.-M. Xu, H. Zhou, K. Ji, F. Chen, J. Zhou and H. Duan, *Angew. Chem. Int. Ed.*, 2022, **61**, e202200211.
34. C. Yang, C. Wang, L. Zhou, W. Duan, Y. Song, F. Zhang, Y. Zhen, J. Zhang, W. Bao, Y. Lu, D. Wang and F. Fu, *Chem. Eng. J.*, 2021, **422**, 130125.
35. B. Zhou, Y. Li, Y. Zou, W. Chen, W. Zhou, M. Song, Y. Wu, Y. Lu, J. Liu, Y. Wang and S. Wang, *Angew. Chem. Int. Ed.*, 2021, **60**, 22908-22914.
36. Y. Sun, J. Wang, Y. Qi, W. Li and C. Wang, *Adv. Sci*, 2022, **9**, 2200957.
37. R. Luo, Y. Li, L. Xing, N. Wang, R. Zhong, Z. Qian, C. Du, G. Yin, Y. Wang and L. Du, *Appl. Catal. B Environ.*, 2022, **311**, 121357.
38. M. Zhou, J. Chen and Y. Li, *Catal. Sci. Technol.*, 2022, **12**, 4288-4297.
39. B. Zhang, H. Fu and T. Mu, *Green Chem.*, 2022, **24**, 877-884.
40. G. Yang, Y. Jiao, H. Yan, Y. Xie, C. Tian, A. Wu, Y. Wang and H. Fu, *Nat. Commun.*, 2022, **13**, 3125.
41. S. Yang, Y. Guo, Y. Zhao, L. Zhang, H. Shen, J. Wang, J. Li, C. Wu, W. Wang, Y. Cao, S. Zhuo, Q. Zhang and H. Zhang, *Small*, 2022, **18**, 2201306.